Development of a Cost-Effective and Consumable-Free Interface for Comprehensive Two-Dimensional Gas Chromatography (GC×GC)

By

Ognjen Panić

A thesis
presented to the University of Waterloo
in fulfillment of the
thesis requirement for the degree of

Master of Science
in
Chemistry

Waterloo, Ontario, Canada 2007

I hereby declare that I am the sole author of this thesis. This is a true copy of the thesis, including any required final revisions, as accepted by my examiners.

I understand that my thesis may be made electronically available to the public.

Abstract

The biggest limitation to conventional gas chromatography (GC) is limited peak capacity, making the analysis of complex mixtures a difficult or even impossible task. Comprehensive two-dimensional gas chromatography (GC×GC) significantly increases peak capacity and resolution, improves sensitivity and generates structured 3D chromatograms. This is achieved by connecting two columns coated with different stationary phases through a special interface (modulator). The interface samples the first column effluent and periodically injects fractions of this material, as narrow injection pulses, onto the second column for further separation. Commercial instruments achieve this with cryogenic agents. Since this expensive approach permits only in-laboratory analysis, the development of simple, economical and field-capable GC×GC systems is in demand.

This report summarizes the fundamentals governing GC×GC separations and a brief history of technological advances in the field. It also documents the construction of a simple interface, devoid of moving parts and cryogenic consumables, and hence highly suitable for field analysis and monitoring applications. Evaluation of the interface suggests on-par performance with more complicated cryogenic modulators. GC×GC separations of technical mixtures of fatty acid methyl esters (FAMEs), common environmental pollutants (EPA 8270), polychlorinated biphenyls (PCBs), pesticides (toxaphene), as well as selected essential oils and major distillation fractions of crude oil indicate very good performance. Most notably, the interface prototype was applied for the first ever time-resolved on-site analysis of the semi-volatile organic fraction of urban air particulate matter ($PM_{2.5}$).

Acknowledgements

I would like to express my deepest and most sincere gratitude to my supervisor, mentor and friend, Dr. Tadeusz Górecki. The journey we enjoyed in the past two years was among the most academically meaningful and personally fulfilling experiences of my life.

Secondly, I would like to thank Dr. Allen Goldstein and his associates at the University of California at Berkeley for their collaboration and the application of the developed GC×GC instrumentation for novel and meaningful investigations.

A project of this scope would not have been possible without the continuous guidance and support from the University's science and technical services (STS). I would especially like to thank Jacek Szubra, Harmen Vander Heide and Andy Colclough for expanding my knowledge outside the boundaries set by traditional chemistry.

Past and present members of our research group have certainly made the difficulties encountered in research more bearable and less serious than they initially seemed. Special thanks go to Dr. James Harynuk for meaningful after-hours GC×GC discussions. I am also thankful to Dr. Ziba Parsi for all of her professional and personal consultation.

Finally, I would like to dedicate this thesis to my family, who continue to support every decision I make.

Table of Contents

Abstract……...iii
Acknowledgments…….. iv
Table of Contents…… v
List of Figures…….…… vii
List of Tables……..…… ix

1.0 Introduction…….…….. 1
1.1 GC×GC Fundamentals……..5
1.1.1 Principles of GC×GC Separations……....5
1.1.2 Interpretation of GC×GC Data…….. 11
1.1.3 GC×GC Instrumentation…….…… 14
1.2 An Evolutionary Perspective on GC×GC Interface Design…... 17
1.2.1 Thermal Interfaces…….. 17
1.2.1.1 Heater-based Interfaces……17
1.2.1.2. Cryogenically-operated Interfaces…….....20
1.2.2 Valve-based Interfaces…….…...24
1.3 Anticipated Direction of Future GC×GC Instrumentation…....26
1.4 References……..…. 29

2.0 Experimental Procedures……33

3.0 Development of the Interface……..40
3.1 Trapping Capillary……..…. 43
3.2 Capacitative Discharge Power Supply……..53
3.3 Cooling Blower……55
3.4 Evaluation of the Interface…….. 58
3.5 Conclusions and Future Considerations…….…..67
3.6 References……..…. 70

4.0 Selected Applications……..72
4.1 Environmental Analysis…… 72
4.1.1 Air Analysis…… 72
4.1.2 Polychlorinated Biphenyls (PCBs) and Pesticides…….... 79
4.2 Essential Oils……...87
4.3 Petrochemical Analysis……89
4.4 Conclusions…… 92
4.5 References…… 93

Appendix……..……...98
References……... 100

List of Figures

Figure 1.1: The steps of an analytical procedure…… 1
Figure 1.2: Block diagram of a GC system…… 3
Figure 1.3: Block diagram of a GC×GC instrument……..……..6
Figure 1.4: The role of the GC×GC interface……..…….. 8
Figure 1.5: Modulation and phasing in preservation of the 1D separation… 10
Figure 1.6: Generation and interpretation of GC×GC data……..... 12
Figure 1.7: Analysis of EPA method 8270 standard mixture…….. 13
Figure 1.8: Heater-based thermal interfaces……..19
Figure 1.9: Longitudinally modulated cryogenic system (LMCS)……..21
Figure 1.10: Dual-stage cryogenic interfaces with no moving parts…… 23

Figure 2.1: Block diagram of the middle mount ……..34
Figure 2.2: Capacitative discharge power supply electronic diagram……....35

Figure 3.1: The proposed GC×GC system……42
Figure 3.2: Schematic diagrams of the trapping capillary…… 44
Figure 3.3: Flattening of the trapping capillaries…….……....47
Figure 3.4: Effects of cold spots on the GC×GC separation……49
Figure 3.5: Selective removal of stationary phase in the trapping capillary .. 51
Figure 3.6: Effects of forced cooling on modulation……....56
Figure 3.7: Vortex tube ……..…… 57
Figure 3.8: Separation of diesel fuel……..…… 60
Figure 3.9: GC×GC analysis of a window defining standard……....63
Figure 3.10: Analyzable volatility range of various interface prototypes……. 64
Figure 3.11: GC×GC analysis of gasoline……..…… 65

Figure 4.1: 2D-TAG analysis of fatty acid methyl esters and EPA 8270….. 77
Figure 4.2: 2D-TAG analysis of ambient air……..... 77

Figure 4.3: Time-resolved on-site 2D-TAG analysis of urban air…….…. 78
Figure 4.4: GC×GC-FID analysis of PCB technical mixtures…… 83
Figure 4.5: GC×GC-FID analysis of transformer oil spiked with PCBs…....84
Figure 4.6: GC×GC-FID separation of toxaphene…….…… 86
Figure 4.7: GC×GC analysis of rosemary, neroli and sage essential oils..... 88
Figure 4.8: GC×GC-FID analysis of semi-volatile petrochemical mixtures..91

List of Tables

Table 2.1: A summary of all experimental conditions……...39

Table 3.1: Evaluation of interface prototypes constructed……..…..46
Table 3.2: Calibration of the capacitative discharge power supply…….. 54
Table 3.3: Comparison of 2D peak widths with various interface types..... 59
Table 3.4: Projected operational costs for various interfaces……..... 66

Table 4.1: Selected GC×GC separations of essential oils……..... 87

1 Introduction

The goal of any analytical procedure is to obtain qualitative and/or quantitative chemical and structural information about compound(s) of interest. Depending on the type of application, this can be a challenging task because analytes in nature are rarely found in their pure state; moreover, they can be part of complex mixtures and/or be present in trace amounts. Hence, the process of chemical analysis usually consists of separation, identification and quantification of compounds from a mixture. In many types of analyses, this procedure consists of sampling, sample preparation, separation and detection (Figure 1.1). Sample preparation pre-concentrates the analytes of interest and removes matrix interferences. Following this, separation of compounds of interest is carried out by the most suitable method. Examples of such separations include capillary electrophoresis (CE), thin-layer chromatography (TLC), high-performance liquid chromatography (HPLC) and gas chromatography (GC). Finally, structural information can be obtained by utilizing ultraviolet (UV), Fourier transform infrared (FTIR), nuclear magnetic resonance (NMR) spectroscopy, and mass spectrometric (MS) detectors. While the effectiveness of all the steps outlined in Figure 1.1 could be enhanced, it is the separation that often limits the success of the analysis.

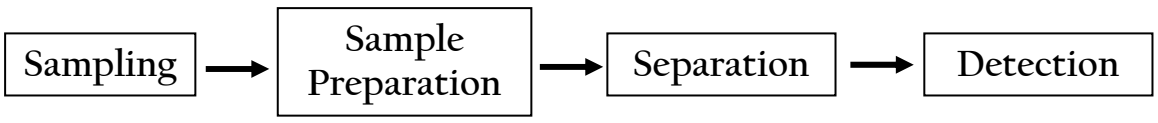

Figure 1.1. *The sequence of events in an analytical procedure.*

Gas chromatography (GC) is presently the most reliable method for analyzing volatile organic compounds (VOCs). The instrumental components of a GC system are illustrated in Figure 1.2. Following the vapourization of the sample in the injector, the carrier gas sweeps the analytes into a column coated with a stationary phase. Separation of analytes occurs inside the column and depends on the partitioning of the compounds from the mobile phase (carrier gas) into the stationary phase (column coating), and vice versa. Ideally, the detector records a chromatogram representing the separated analytes as peaks characterized by elution time (retention time) and signal intensity. In reality, however, complex samples usually contain many closely eluting compounds and matrix components, exceeding the peak capacity in one chromatographic dimension (1D) [1]. The resulting chromatogram can contain many co-eluting peaks and/or unresolved regions, which leads to poor analyte identification and quantification. Poor chromatographic resolution can be compensated with more effective sample preparation procedures and more selective detection systems. For example, pre-chromatographic treatment of many complex mixtures requires expensive, labour-intensive and selective sample preparation methods [2]. Even when coupled to MS detectors capable of mass spectral deconvolution of overlapping peaks, such as the time-of-flight mass spectrometer (TOF-MS), unresolved chromatograms can cause poor analyte separation and inconclusive structural identification. In such cases, it may be necessary to use high resolution mass spectrometry (HRMS), which is very expensive [2].

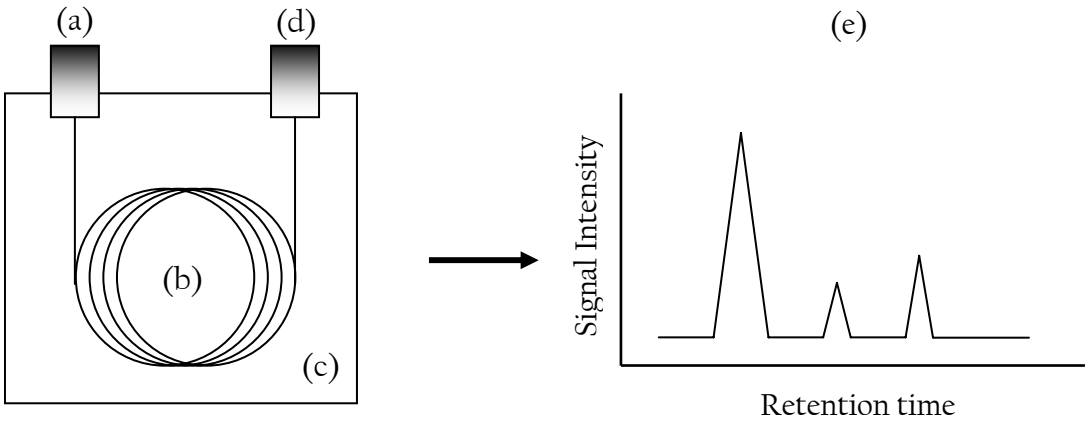

Figure 1.2: *Block diagram of a GC instrument, consisting of (a) injector, (b) column, (c) oven, and (d) detector, which generates (e) the chromatogram.*

As commercially available capillary columns are coated with stationary phases that separate analytes based on a prevailing separation mechanism (volatility, chirality, etc.), the inability to fully resolve complex samples is experienced in many different areas. For example, the petroleum industry requires rapid characterization of different petroleum fractions; the food and fragrance industry, as well as the environment and health sectors both depend on the analysis of trace amounts of analytes in complex matrices; and finally, the forensic sector is in need for reliable methods capable of pattern recognition in complex samples [3]. Realizing the potential gain in resolution, Giddings first introduced the concept of multidimensionality in gas chromatography in 1984 [4]. He predicted that subjecting a sample to two different separation dimensions (columns coated with different stationary phases) would dramatically increase the peak capacity in GC. Giddings defined a comprehensive multidimensional separation as one in which an entire sample is subject to separation in all separation dimensions (comprehensive) and one in which all previous separations are preserved (multidimensional). However, he

failed to pragmatically demonstrate comprehensive two-dimensional gas chromatographic separations [4].

The peak capacity problem in conventional GC was initially approached by performing multi-dimensional gas chromatography (MDGC) [5]. In this approach, also termed "heart-cutting", only a fraction, or several fractions, of an unresolved chromatogram were injected into a second column coated with a different stationary phase. With respect to environmental analysis, early applications using heart-cutting resulted in improved separations of many samples, including polychlorinated biphenyls (PCBs), pesticides, and toxaphene [6,7,8,9,10,11]. Nevertheless, automation in MDGC is difficult and the method increases the resolution for only a fraction of the entire chromatogram. The dream of a comprehensive multidimensional GC method became reality in 1991, when John Phillips integrated a simple interface (modulator) between two columns and constructed the first comprehensive two-dimensional gas chromatographic system (GC×GC) [12].

For the next sixteen years, the development of a variety of interface designs caused a rapid increase in the number of applications dealing with petrochemical, environmental, health, food and fragrance, and forensic analyses. GC×GC is currently considered as one of the most powerful analytical tools for the analysis of VOCs, offering increased peak capacity and resolution, enhanced sensitivity, and structured two-dimensional (2D) chromatograms (see Figure 3.8).

1.1 GC×GC Fundamentals

1.1.1 Principles of GC×GC Separations

The concept of a comprehensive multidimensional separation for the purpose of increased resolution is not unique to gas chromatography; in fact, it has been successfully used in planar chromatography for a long time. For example, thin-layer chromatography (TLC) requires a drop of an unknown mixture to be placed in one corner of the TLC plate before developing the plate [13]. While the mobile phase transports the components of the mixture upward, separation of the analytes is based on the interactions between the mobile phase (solvent) and the stationary phase (plate). The resulting chromatogram consists of separated spots along a vertical line. A multidimensional separation is accomplished by drying the plate, rotating it by 90° (so that the previously separated species fall along a horizontal line at the bottom) and developing the plate with a different mobile phase. Consequently, the spots from the first analysis are further separated during the second TLC plate development. Another prime example of a multidimensional method is 2D sodium dodecyl sulfate polyacrylamide gel electrophoresis (2D-SDS-PAGE), a revolutionary and invaluable separation tool utilized in biological applications and research. In this method, proteins are separated based on their isoelectric point (pI) in the first dimension and according to their molecular weight (MW) in the second dimension. Both 2D-TLC and 2D-SDS-PAGE are examples of comprehensive multidimensional separations in which the two separation dimensions applied in each method are orthogonal, or independent of each other.

Orthogonality in gas chromatography can be accomplished by using two columns whose stationary phases exhibit different selectivity towards the analytes, e.g. one column separating analytes based on their volatility, and the other based on volatility and polarity [14]. The concept of a comprehensive two-dimensional separation, however, is experimentally more challenging to implement. This difficulty arises from the fact that the separation in GC is carried out in time, while in planar chromatography (TLC) it is carried out in space; hence, the only way to achieve a comprehensive two-dimensional chromatographic separation is to join the two columns with a special interface [3].

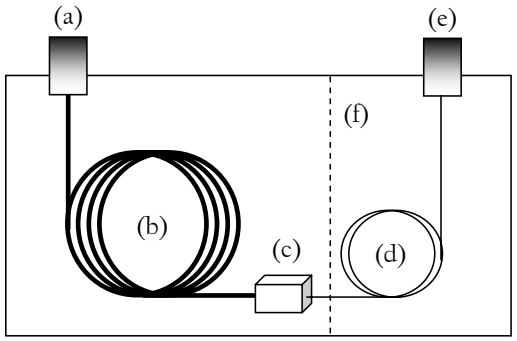

Figure 1.3: *Block diagram of a GC×GC system; (a) injector; (b) primary column; (c) interface, or modulator; (d) secondary column; (e) detector; (f) optional secondary oven [1].*

Typical instrumental components of a GC×GC system are illustrated in Figure 1.3. Considered the heart of the method, the modulator periodically traps, focuses and injects fractions of the primary dimension effluent into the secondary column for further chromatographic analysis. This must be performed at a rate that permits the preservation of the primary dimension separation. To achieve this, the interface traps analytes from the first dimension for a short period of time, and then injects a fraction of those analytes into the second dimension column as a narrow

pulse. Following the completion of the separation in the secondary column, another fraction of the 1D column effluent is injected in the second dimension column. This process is repeated throughout the entire GC×GC analysis. Consequently, the detector records a continuous chromatogram consisting of short sequential two-dimensional (2D) chromatograms.

The requirement for the interface is justified in Figure 1.4 [1]. A hypothetical mixture of three compounds is separated into its respective components in the first dimension column (Figure 1.4 A). Upon entering the second column, coated with a different stationary phase, the relative rates of migration change. Consequently, co-elutions of previously separated bands (Figure 1.4 B) and changes in the elution order (Figure 1.4 C) are likely. Overall, the separation obtained in the first dimension is not preserved, and might actually be degraded. Thus, connecting two orthogonal columns in series is equivalent to using a single dimension separation on a column with a mixed stationary phase [1].

Subjecting the same hypothetical mixture to two columns joined by an interface prevents the continual flow of analytes into the secondary column (Figure 1.4 D). Instead, the modulator traps and focuses the black band and then injects it as a narrow pulse into the 2D column (Figure 1.4 E). In the meantime, the modulator traps and focuses the gray band until the black band has reached the detector (Figure 1.4 F). Lastly, the spotted band replaces the gray band in the interface, and is not injected until the separation of the gray band into two separate compounds is complete (Figure 1.4 G). Therefore, the integration of an interface between two

columns preserves the separation achieved in the first column and allows for extra separation in the second column [1].

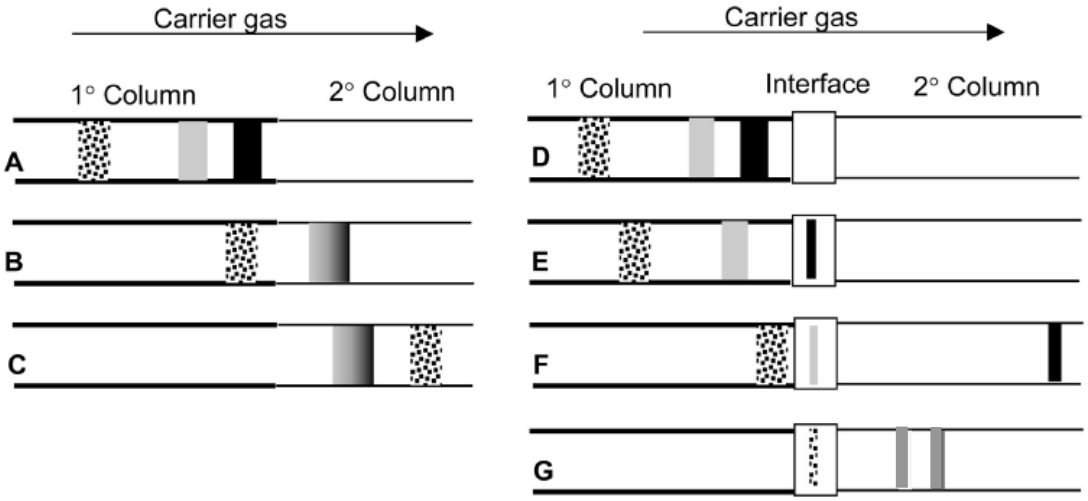

Figure 1.4: *The need for the GC×GC interface. (A-C) Connecting two different columns in series can cause peak recombination and an overall change in elution order. (D-G) An interface between the two columns injects a fraction of the analytes from the first column into the second column as a short chromatographic pulse, while trapping the remaining fractions [1].*

Preservation of the primary dimension separation depends on the frequency of modulation. It has been demonstrated that each peak entering the interface must be sampled at least three times, although 2.5 times has been suggested recently [15,16]. This implies that an 18 s wide peak exiting the primary column should be sampled every 6 s. The three-cuts-per-peak approach to preserving primary dimension chromatograms was verified with a mathematical model illustrated in Figure 1.5 [1]. Figures 1.5 A and D are identical and represent hypothetical 1D-GC chromatograms. The simulated modulation was capable of trapping all material entering the modulator in the specified modulation period (i.e. 6 s) and releasing all contents into the second dimension. Accordingly, this required integrating the area

under the 1D curve and displaying it as a 2D injection pulse (i.e. for intervals 0 - 6 s, 6 - 12 s, etc.). To account for the mass compression of analyte fractions by the modulator, the original chromatogram was magnified and plotted as a dotted curve (Figure 1.5 B-F). The 2D pulses produced by the modulator were joined by their apexes (marked with circles) with a dashed line as a means of reconstructing the original chromatogram [1]. Finally, the effect of the modulation period on the preservation of the primary dimension separation was tested by comparing an acceptable modulation period of 6 s (Figure 1.5 B), and a sub-optimal modulation period of 12 s (Figure 1.5 E) on the preservation of 24 s wide 1D peaks. It is evident that sampling a peak only two times (Figure 1.5 E) leads to a less accurate reconstruction of the 1D chromatogram, and separation accomplished in the first dimension can be lost (see the 2nd and 3rd peak).

The phase of modulation (Φ) has an affect on the appearance of the reconstructed primary dimension separation. Phasing is an instrumental parameter that can be defined as the time difference between the start of the chromatographic analysis and the commencement of modulation. Marriott et al. defined phasing as the position of the modulator pulses relative to the peaks exiting the 1D column [17]. For example, when comparing an analysis with simultaneous injection and modulation times (Figures 1.5 B and E), i.e. phasing of 0 s, to one where modulation started 3 s after injection (Figures 1.5 C and F), i.e. phasing of 3 s, it becomes evident that the shape of the original chromatogram is altered. If not accounted for, the phase of modulation can cause variations in the appearance of GC×GC chromatograms. Fortunately, phasing effects can be eliminated by integrating a

common start/stop function for both the modulator and the GC; in this event, modulation and sample injection would start simultaneously and reproducibly.

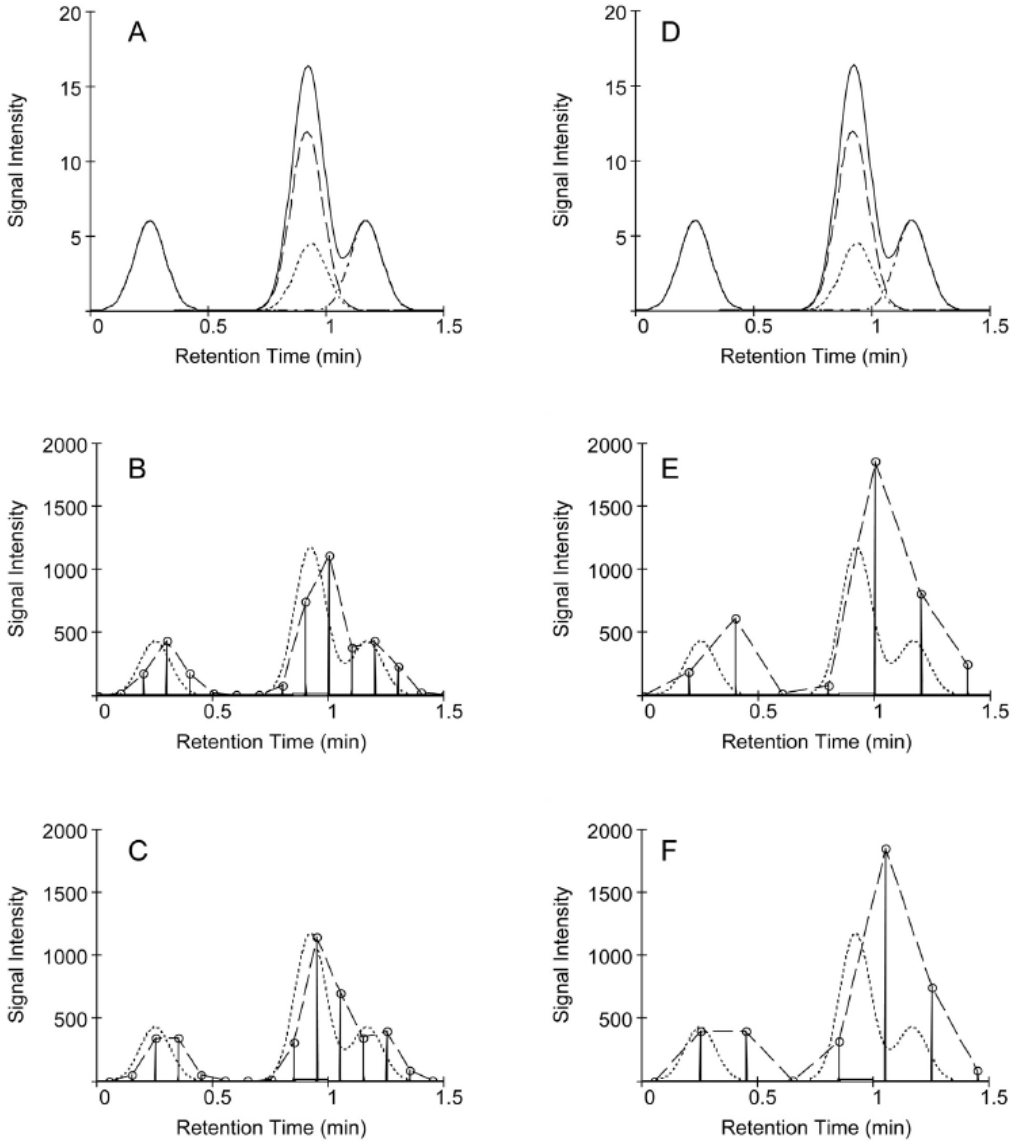

Figure 1.5: *The effect of the modulation period (P_M) and phasing (Φ) on the preservation of the 1D separation. (A and D) Hypothetical 1D chromatograms with peak widths of 24 s; (B) reconstructed 1D chromatogram with a P_M = 6 s and Φ = 0 s; (C) reconstructed 1D chromatogram with a P_M = 6 s and Φ = 3 s; (E) reconstructed 1D chromatogram with a P_M = 12 s and Φ = 0 s; (F) reconstructed 1D chromatogram with a P_M = 12 s and Φ = 3 s. For visual comparison, the original 1-D chromatogram is magnified 72 times and plotted as a dotted line, while the reconstructed 1D chromatogram is plotted as a dashed line [1].*

Interface performance can be evaluated by the width of peaks presented to the second dimension. Ideal modulators should generate very narrow peaks, with optimal values at half height below 150 ms [17,18]. The reason for this is that peak capacity is dramatically increased when peak widths in the second dimension are narrower. Furthermore, narrower peaks are characterized by higher signal intensity, consequently decreasing the detection limits. This gain in sensitivity depends on the modulator type and modulation frequency, as well as the separation in the secondary column. Increased signal intensity is observed with modulators that collect (focus or compress) rather than sample the primary dimension effluent (see section 1.2).

1.1.2 Interpretation of GC×GC Data

In a GC×GC method, fractions of 1D column effluent are periodically injected, as narrow pulses, into the second column; consequently, the data is recorded as a continuous chromatogram consisting of a series of short second dimension separations [19]. Each peak eluting from the first column should be modulated at least three times; therefore, each component responsible for the peak is present in at least three consecutive secondary dimension chromatograms, frequently termed "slices". Clearly, this approach to data presentation is uninformative and perplexing, and requires computer processing before useful interpretation is possible.

The process of GC×GC chromatogram generation is illustrated in Figure 1.6 [1]. First, appropriate computer software slices the original chromatogram (Figure 1.6 A) according to the specified modulation period ($t_2 - t_1$, $t_3 - t_2$, etc.). At this time, first dimension retention times are defined as the times when injection into the

second column (t_1, t_2, t_3, etc.) occurred (Figure 1.6 B). The 2D retention times are determined by subtracting the primary dimension retention time from the original retention time [20]. Once the individual second dimension slices have been identified by the computer software, the next task is to line them up side by side and generate a three-dimensional (3D) plot. Figure 6 C illustrates that such a plot consists of the 1D retention time as the x-axis, the 2D retention time as the y-axis and the signal intensity as the z-axis. Although 3D GC×GC plots are useful when working on the computer screen, they are easier to interpret on paper when plotted top-down, as a contour plot (Figure 1.6 D). In this fashion, the first and second dimension retention times are plotted on the x- and y-axes, respectively, while signal intensity is either colour-coded or represented with contour lines. An example of a contour plot is illustrated in Figure 1.7.

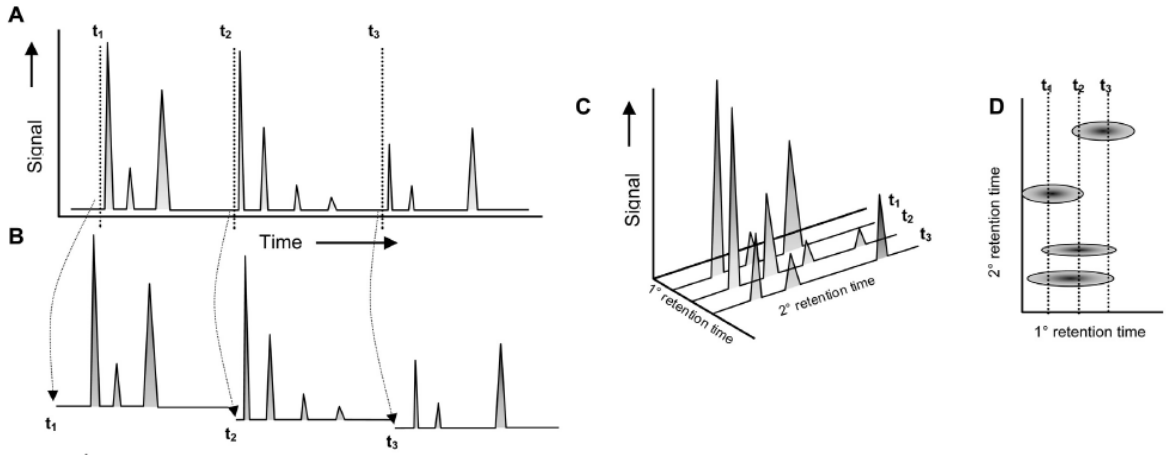

Figure 1.6. *Generation and interpretation of GC×GC data. (A) the original chromatogram consists of a series of short second dimension chromatograms; (B) slicing individual second column chromatograms by the computer software is based on the modulation period; (C) aligning individual slices to generate a 3D GC×GC plot, with 1st retention time (x-axis), 2nd retention time (y-axis) and signal intensity (z-axis); (D) the top-down view of the 3D plot produces the contour plot, where, 1st and 2nd retention times are the x-and y-axes and the signal intensity is colour coded [1].*

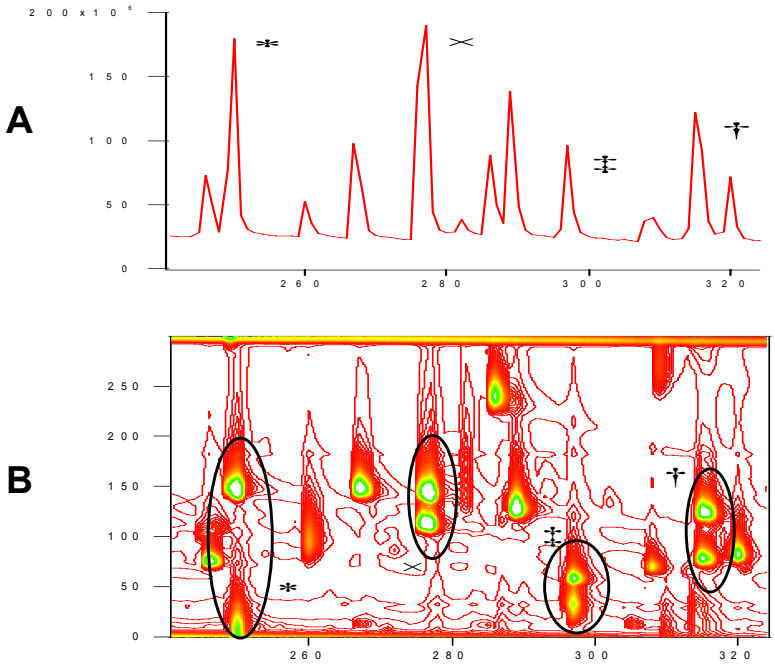

Figure 1.7. *Analysis of EPA Method 8270 standard mixture, containing 116 of the most common pollutants of air, water and soil. In only a fraction of the chromatogram, co-elutions appearing as normal peaks in 1D-GC (marked in A) are fully separated in GC×GC (marked and circled in B).*

The structure of a GC×GC chromatogram can be degraded when the elution time of a compound exceeds the modulation period. In such cases, a second dimension peak seems to elute at the beginning of the next slice after data conversion into the 3D plot. Such peaks are often referred to as "wraparound" peaks (e.g. see the circled peak in Figure 4.2). Although wraparound peaks can cause co-elutions and can degrade the ordered nature of a GC×GC chromatogram, they are relatively easy to identify [21]. Their longer elution times cause significant band broadening in the second column, making them broader than the surrounding, non-wrapped peaks.

Quantification of GC×GC data requires individual integration of all peaks related to a particular analyte, followed by their summation [22]. For example, since each 1D peak will be subjected to at least three secondary separations, the raw

GC×GC chromatogram will contain at least three peaks representing the analyte of interest. Each of those peaks must be integrated individually, and the areas of all the peaks then summed to produce the total area of the peak.

Analyte identification in comprehensive 2D-GC is more reliable than in conventional GC (1D-GC) because each analyte can be identified on the basis of two retention times (Figure 1.7). Considering the use of two orthogonal columns, a single GC×GC analysis is representative of two independent 1D-GC analyses. Secondly, and more importantly, GC×GC generates highly structured chromatograms, perfectly suitable for monitoring (environmental analysis) and pattern recognition (forensics) applications [23]. Homologous groups of compounds appear as distinct bands in the contour plot, making rapid and positive identification possible merely by visual inspection. The petroleum industry has benefited from this advantage the most, as compound groups such as alkanes, alkenes, aromatics, to name a few, reproducibly appear in distinct regions of the separation space (see Figure 3.8 C).

1.1.3 GC×GC Instrumentation

Most traditional components utilized in conventional GC are compatible with GC×GC systems. With respect to injection and injection techniques, any method suitable in GC can in essence be applied to comprehensive two-dimensional gas chromatography.

Column selection in GC×GC plays an important role in the success of the separation. First dimension columns are usually long (15 – 30 m), narrow bore (0.25 mm inner diameter {ID}) and are preferably coated with a thick layer of a stationary phase (0.25 μm – 1 μm) [19]. They generate peak widths first dimension that permit the preservation of the 1D separation with typical modulation periods of 3 – 6 s. Conventionally, columns in the first dimension are coated with non-polar stationary phases, such as 100 % polydimethylsiloxane (PDMS) or 95/5 % methyl/phenyl siloxane [19]. Since the modulation period limits the separation time in the second dimension, it is not surprising that 2D columns must be efficient and fast. Common second columns are short (0.5 – 1.5 m), narrow bore (0.1 mm ID) and are coated with a thin film of a stationary phase (0.1 – 0.25 μm). Although higher efficiency is obtained by using 0.1 mm ID columns, modulators capable of compressing injection pulses make these columns prone to overloading. Hence, it has been suggested that thin-film 0.25 mm ID secondary dimension columns might be optimal for at least some GC×GC separations [24,25]. To ensure an orthogonal separation, the selectivity in the second dimension must differ from that in the first dimension. The most typical GC×GC methods utilize 2D columns that are coated with 50/50% phenyl/methyl or "wax" (polyethylene glycol)-based stationary phases [19]. In this way, the first column separates compounds based on volatility, while the second column separates compounds predominantly based on their polarity.

In many commercially available GC×GC systems the second column is enclosed in a separate oven (Figure 1.3 e). Although this allows for greater flexibility during method development, it is not a necessity. In fact, many research laboratories

operating home-made GC×GC instruments keep both columns in the same oven to prevent the additional complexity.

The range of detectors suitable for GC×GC is not as broad as in conventional GC methods. Recalling that the secondary column produces short chromatograms with peak widths on the order of 150 ms or less, suitable detectors must be characterized by fast data acquisition rates. For instance, collecting at least 10 data points along such narrow peak profiles requires detectors with sampling rates of at least 70 Hz [3]. A combination of fast data acquisition and low cost places the flame ionization detector (FID) among the most commonly used in GC×GC. However, applications utilizing the electron capture detector (μ-ECD) [26,27], sulphur chemiluminescence detector (SCD) [28], nitrogen chemiluminescence detector (NCD) [29], and the atomic emission detector (AED) [30] have been reported.

Mass spectrometry (MS) is presently the most powerful and most informative detector in chromatography. In fact, when hyphenated to GC, MS detectors generate another separation dimension. Presently, the most commonly used MS detector in GC×GC is the time-of-flight mass spectrometer (TOF-MS). Its fast data acquisition rates, allowing the acquisition of up to 1 000 spectra per second, and its ability for spectral deconvolution of chromatographically unresolved peaks make GC×GC–TOF-MS systems one of the most powerful tools for the separation of volatile and semi-volatile mixtures.

As the interface remains the core of the method, it is not surprising that a tremendous amount of research effort was initially invested in its design and development. This has led to the emergence of two classes of interfaces, thermal

and valve-based modulators. The more popular thermal interfaces can modulate based on an increase in temperature (heater-based), or based on a decrease in temperature (cryogenic). Alternatively, the approach to modulation utilizing valves relies on periodically venting the majority of 1D flow and subjecting the remaining fraction to separation in the second column. The following section will briefly summarize the technological advances made in the field of GC×GC interface design.

1.2 An Evolutionary Perspective on GC×GC Interface Design

1.2.1 Thermal Interfaces

1.2.1.1 Heater-based Interfaces

In 1991, Liu and Phillips developed the first GC×GC modulator [12]. This interface was very simple and consisted of a segment of a thick-film fused silica capillary, with the outer surface coated with gold paint. Residing between two GC ovens, the interface would trap and compress analyte bands exiting the primary column via partitioning into the stationary phase. Injecting these analytes into the second column was periodically achieved by ohmically heating the gold-painted trap. The results obtained with this interface, however, were not satisfactory. More specifically, the injection bands onto the second column were broad and irregular. Recognizing that heating the entire interface as a single component caused analyte breakthrough, Phillips eliminated this obstacle by implementing two sequential heating segments [12]. His dual-stage trap, illustrated in Figure 1.8 A, was a success at the time. Analytes entering the first segment of the interface (1 in Figure 1.8 A)

were trapped, compressed, and then remobilized by briefly heating the capillary between points x and y, and finally re-trapped and re-compressed in the cooler second segment of the modulator (2 in Figure 1.8 A) [3]. Once segment 1 cooled, it would trap analytes again, at which time the trapped analytes in the second segment were desorbed and injected into the second column via heating the capillary between points y and z. This cycle was repeated throughout the entire analysis. It is important to note that even though this pioneering interface technology was not very robust and faced reproducibility issues, it provided proof of concept in the field of GC×GC, and illustrated that dual-stage modulation is mandatory.

Later, Phillips developed and commercialized the rotating thermal modulator [31,32]. Similar to his first model, trapping and focusing of analytes exiting the primary dimension was accomplished with a thick-film capillary. However, instead of using direct resistive heating to remobilize and inject the analytes into the secondary column, a rotating thermal heater was implemented (Figure 1.8 B). The motion of the heater re-mobilized the trapped analytes from primary column and propagated this band downstream to a cooler segment of the trapping capillary. At this point, a narrow injection band formed and was injected into the secondary column while other analytes were trapped upstream, at oven temperature. The rotational movement of the thermal heater was repeated throughout the entire analysis. This modulator proved to be more robust and applicable to a number of different applications, but it suffered from limitations related to the presence of moving parts and to inefficient trapping of volatile compounds.

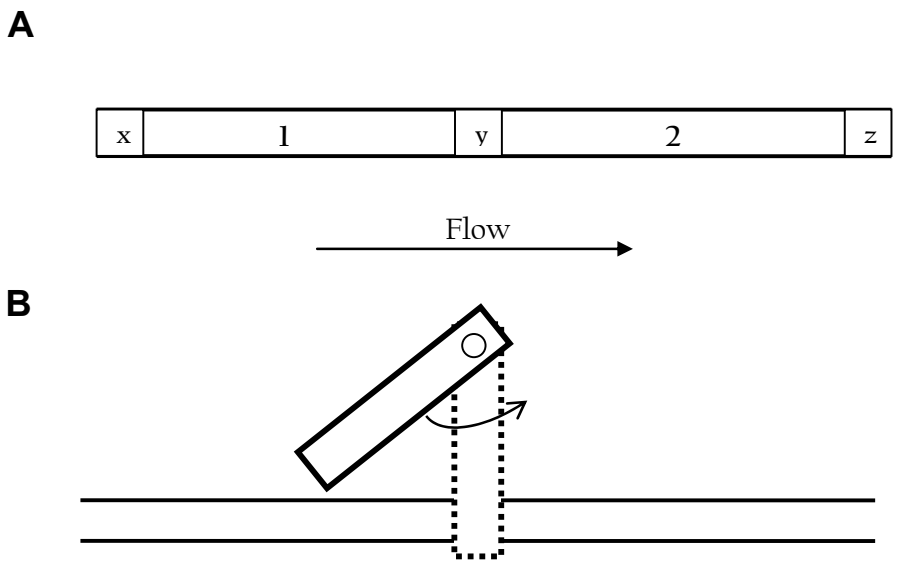

Figure 1.8. *Heater-based thermal interfaces designed by Phillips. (A) The original dual-stage modulator utilized periodic and alternative resistive heating of segments 1 and 2 for analyte trapping and desorption. (B) The rotating thermal sweeper, heated to approximately 100° C above oven temperature, re-mobilized fractions of primary column effluent in the thick-film trapping capillary with its periodic angular motion [3].*

One of the first interfaces developed in our laboratory consisted of a Silcosteel® capillary filled with a micro sorbent bed [33]. The inline sorbent trapped analytes eluting from the first dimension; injections into the secondary column were achieved by ohmically heating the Silcosteel® capillary. This approach to modulator design eliminated moving parts and increased the trapping capacity (sorbent bed can trap more analytes than a thick-film capillary); however, trapping volatile compounds was ineffective and the sorbent bed was thermally sensitive.

Burger et al. also developed a thermal heater-based interface that consisted of a thick-film capillary column encased by a steel jacket [34]. Instead of dual-stage trapping, the authors employed a multi-stage trapping sequence that mimicked the

rotating heater. Accordingly, this modulator utilized a series of multiple trapping and desorption sequences prior to injection into the secondary column. As with all other heater-based modulators, this one was also ineffective for trapping volatile compounds.

The inability of heater-based modulators to effectively trap volatile compounds and to quickly release semi-volatile compounds at the allowed desorption temperatures led to their discontinued use. Presently, most GC×GC systems are equipped with dual-stage cryogenic interfaces.

1.2.1.2 Cryogenically-operated Interfaces

While John Phillips promoted the use of heater-based modulators in the USA, Australia's Phillip Marriott developed the first cryogenic interface, known as the longitudinally modulated cryogenic system (LMCS). This approach to interface design achieved analyte trapping and focusing at low temperatures [35]. Illustrated in Figure 1.9, the LMCS was a liquid CO_2-cooled movable interface installed at the end of the 1D column. Initially, analytes reaching the trapping position (T in Figure 1.9) would be immobilized and trapped by the cryogenically-cooled interface. Moving the trap upstream into the release position (R in Figure 1.9) re-mobilized the analytes in the T zone, injecting a narrow band into the second column; simultaneously, analytes in the upstream R position were trapped. Returning the trap into the T position caused re-mobilization of analytes in the R zone. The periodic movement of the trap was repeated throughout the entire analysis. This

dual-stage cryogenic modulator had two distinct advantages over its heater-based predecessor: first, it made effective analysis of more volatile analytes possible; second, it extended upper temperature range because modulation was not carried out above oven temperatures [19].

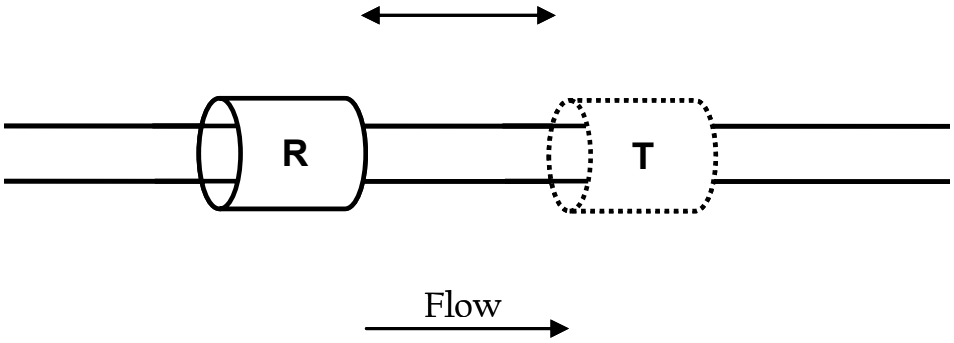

Figure 1.9. *The longitudinally modulated cryogenic system (LMCS). Moving the liquid CO_2-cooled interface allowed sequential trapping (T) and releasing (R) of analytes in the T position and in the R position, alternatively. This repeated process achieved dual-stage cryogenic modulation [3].*

The advantages offered by LMCS persuaded researchers in the GC×GC field to focus their efforts on cryogenic interfaces. The next goal in modulator development became the simplification of the design through elimination of moving parts. Harynuk and Górecki were among the first to construct a cryogenic modulator without any moving parts [33,36]. The proposed modulator consisted of two Silcosteel® capillaries, connected in series, and housed in a chamber cooled with liquid N_2. Since this configuration promoted constant analyte trapping, dual-stage re-mobilization of analytes was accomplished by alternatively and rapidly heating the two capillary segments.

In 2000, Ledford and Billesbach reported the development of a cryogenic modulator with no moving parts [37]. Figure 1.10 A illustrates that their interface

traps analytes via two cold CO_2 jets (C_1 and C_2 in Figure 1.10 A), and consequently re-mobilizes them with two hot air jets (H_1 and H_2 in Figure 1.10 A). Upon commercialization, the LECO Corporation replaced liquid CO_2 with liquid N_2 in order to more effectively trap the most volatile analytes. Later, Beens et al. simplified Ledford's original modulator design by removing the hot air jets [38]. Instead, re-mobilization of analytes in both segments of the trap became a function of the GC oven (Figure 1.10 B). This interface is currently commercially available from the Thermo Electron Corporation. Following this, Ledford et al. further simplified their original modulator by demonstrating dual-stage modulation with one cold gaseous N_2 jet [39]. The single cryojet performed the task of a dual-stage modulator by trapping the same analytes upon exiting the primary dimension column and the delay loop (Figure 1.10 C). Presently, this is the simplest commercially available cryogenic modulator on the market. However, the limitation of this interface in non-routine analysis is that successful operation of this modulator requires that the user precisely adjusts the carrier gas velocity and the length of the delay loop when altering chromatographic parameters.

Shortly thereafter, Harynuk and Górecki also developed a dual-stage, single jet cryogenic modulator with a delay loop [40]. However, instead of using cooled gaseous N_2, trapping analytes was accomplished with a spray of liquid N_2. This allowed for effective modulation of the most volatile analytes, including propane. In addition, the system was equipped with a cost-effective cryogen delivery savings system, consuming ca. 20 L/day of liquid N_2 in comparison to the average consumption rate of 50 to 100 L/day by commercially available systems.

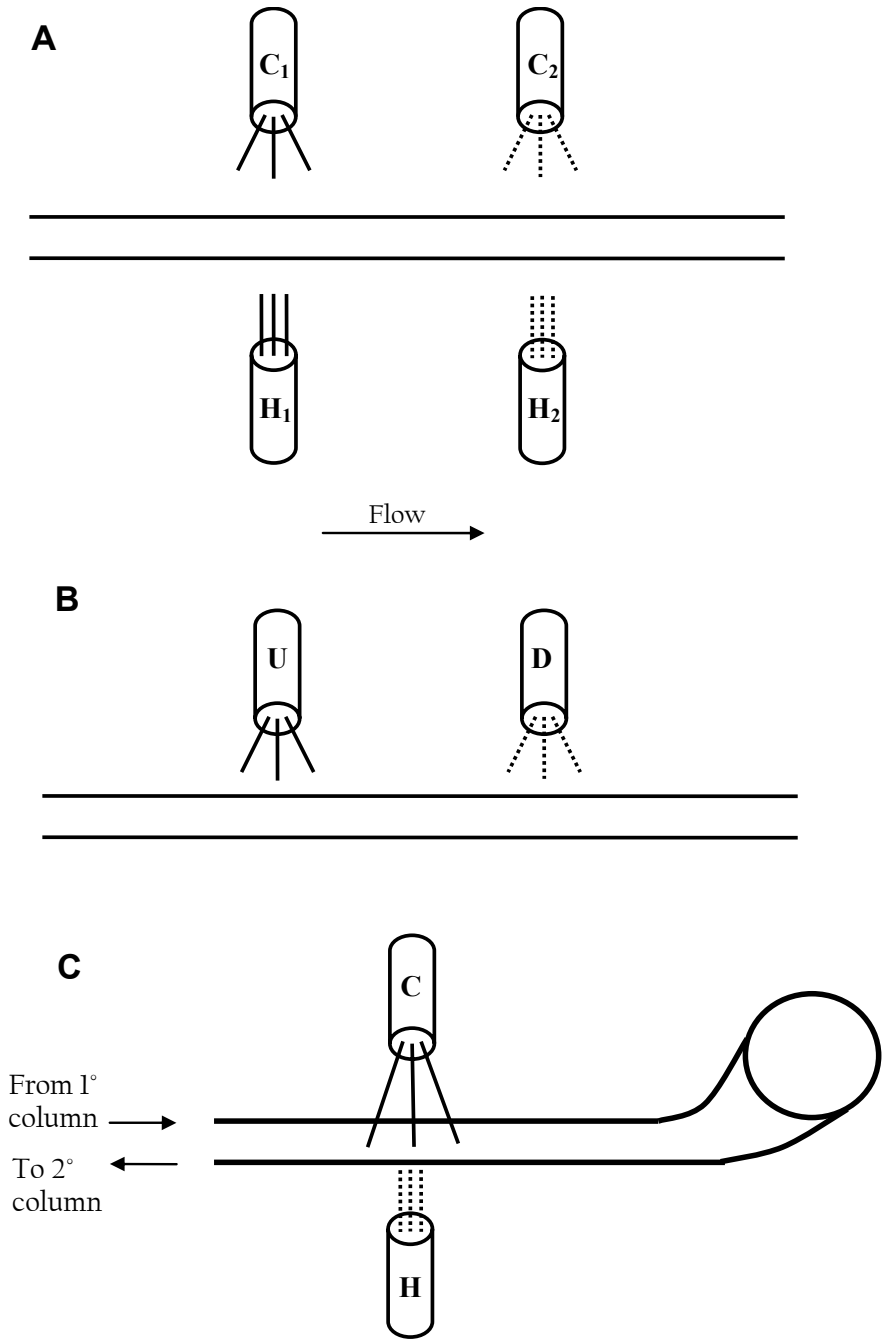

Figure 1.10. *Dual-stage cryogenic interfaces with no moving parts. (A) Dual liquid CO_2 and hot air jet interface developed by Ledford and Billesbach – first commercialized by the Zoex and then the LECO Corporation [37]. (B) Dual liquid CO_2 jet with no hot air jets constructed by Beens et al. – commercialized by the Thermo Electron Corporation [38]. (C) Dual-stage cryogenic interface developed by Ledford and Billesbach – commercialized by the Zoex Corporation [39] – a similar design is used in the Harynuk and Górecki cryogenic interface [40].*

The latest development in cryogenic interface design was reported by Sacks et al.. Revisiting the concept of a cryogenically-cooled chamber housing the trapping capillary, initially invented by Harynuk and Górecki [33], Sacks et al. simplified the design by replacing the liquid N_2 with cold air and utilizing a single-stage resistively heated trapping capillary [41]. This particular interface was incapable of modulating very volatile compounds, as the trapping temperature was only ca. -30 ˚C. The authors improved the cooling efficiency of the trapping capillary, and thus the modulation of the more volatile analytes, by replacing the cool air supply with refrigerated polyethylene glycol (PEG) [42]. While this approach to interface design is characterized by low investment and operating costs, it requires the constant pump-operated circulation of the PEG coolant through the trapping chamber, which is prone to leaks.

1.2.2 Valve-based Interfaces

Around the same time that Marriott developed his LMCS interface, Synovec et al. pioneered modulation by using valves. Using 4 ports of a 6-port diaphragm valve, this interface had two modes of operation: sampling, during which primary column effluent entered the secondary column; and venting, during which primary column effluent was released into the atmosphere, and the secondary separation was performed at high flow rates with an auxiliary gas supply [43]. Compared to cryogenic modulators, this interface did not contribute to increased sensitivity because it lacked the ability to compress analyte bands, and it vented 80 – 90 % of

the sample into the atmosphere. In addition, the diaphragm valve lowered the upper temperature limit of the GC×GC temperature program.

Later, Seeley et al. constructed an interface which utilized all 6 ports of a diaphragm valve with the addition of a sample loop [44]. In this approach, primary column effluent filled the sample loop before being vented into the atmosphere. Switching the valve to the sampling position caused the analytes in the sample loop to be compressed before injection into the secondary column. Sampling was completed by switching the valve back to the venting position, allowing the separation in the second dimension to be rapidly performed via auxiliary gas flow. This version of the valve-based modulator enhanced sensitivity as it exhibited some mass compression, and because it sampled approximately 80 % of the first dimension column effluent. Unfortunately, this modulator did not resolve the limitation of low upper temperature limits associated with diaphragm valves.

Seeley et al. eliminated the problems experienced with diaphragm valves at high temperatures by developing an interface which used two sample loops and a pneumatic switching system [45]. Both sample loops were filled with primary column effluent; however, while contents of one loop were injected into the secondary column, the other loop was simultaneously filled with primary dimension effluent. Once the latter occurred, a pressure balancing switch outside the oven (i.e. solenoid valve) forced the effluent from the other loop into the second column; during this time the first sample loop filled with analytes once again. Although this prototype was the first valve-based interface capable of 100 % sampling rate and mass compression, it was limited to relatively short modulation periods (2 s or less)

[45]. In spite of the reduced peak capacity caused by short modulation periods, this modulator was successfully applied for the analysis of gasoline, a relatively volatile and complex mixture [46].

Recently, Kochman et al. utilized Seeley's latest valve-based modulator in combination with a quadrupole MS (QMS) detector, equipped with the supersonic molecular beam (SMB) [47]. Invented by Amirav, SMB is a GC-MS interface that generates more intense molecular ion peaks [48]. The GC×GC–QMS system represents one of the most affordable instruments up to date and is capable of analyzing both volatile and non-volatile mixtures. Unfortunately, its limitations include short modulation periods, a narrow range of feasible carrier gas flows, leak-prone interface installation procedures and difficult method development.

1.3 Anticipated Direction of Future GC×GC Instrumentation

The initial stages of GC×GC research involved a diverse and intense period of productivity devoted to interface design and development. Presently, cryogenically-assisted modulation is considered the most effective and has in fact contributed to a wide variety of applications - which are growing each year. Commercial GC×GC systems, offered by the LECO, Thermo Electron, and Zoex Corporations are not universal in nature; indeed, every modulator is characterized by distinct advantages and limitations. All these instruments are expensive (ca. $75 000 - $100 000 CAD), especially if equipped with the TOF-MS detector (ca. $250 000 - $300 000 CAD). In addition, the constant requirement for cryogenic consumables limits these

instruments to in-laboratory analyses and makes them costly to operate. Thus, it is likely that the transition of GC×GC instrumentation from the research sector into the routine laboratory will depend on the development of systems that are simple, robust, affordable, operationally cost-effective, devoid of cryogenic consumables and applicable to field analysis.

Developments of GC×GC instrumentation with at least some of the aforementioned characteristics have recently been reported. For instance, one way to reduce the overall cost of GC×GC instrumentation is to replace the TOF-MS detector. Modern, fast-scanning quadrupole mass spectrometers have scan rates as high as 10 000 amu/s, making them feasible for some GC×GC applications. Studies utilizing GC×GC–QMS have been reported by Beens and Brinkman [49], Kochman et al. [47] and Song et al. [50]. All these applications compromise performance for lower prices, as mass spectral information can only be obtained for narrow mass ranges (i.e. 50 – 250 amu) [3].

Significant changes in the field of GC×GC instrumentation will primarily depend on refocusing research efforts towards the development and engineering of the interface. Ironically, the two interface classes that are presently considered inferior to cryogenic modulators, i.e. heater- and valve-based, have the potential to aid the transformation of GC×GC into a routine analytical tool. For example, the most recent advance in interface design was demonstrated by Seeley et al. [51]. The operational principles of this interface are based on valve-based modulation; however, flow regulation for the purpose of sampling 1D effluent is accomplished with a commercially available Deans switch, rather than a 6-port diaphragm valve.

The Deans switch is a two-state microfluidic flow switching device that can rapidly divert the direction of gas flow from one pathway to another [52]. With regards to GC×GC, Seeley et al. illustrated that the Deans switch can be used as an interface in the following manner: in the sampling state, first column effluent is injected onto the 2D column through a pressure pulse from an externally installed solenoid valve; in the bypass state, first column gas flow is rapidly diverted away from the second column and is temporary stored and compressed in a segment of uncoated fused silica capillary; finally, the aforementioned portion of the 1D effluent is injected onto the 2D column during the next sampling stage [51]. This approach to interface design represents the simplest and cheapest modulator yet reported, and is characterized by: installation simplicity, low manufacturing and operational costs, the absence of moving parts and consumables, the ability to perform on-site analysis and indiscriminate modulation based on analyte volatility. Unfortunately, trace analysis in really complex mixtures is not optimal because the Deans switch interface is limited to relatively short modulation periods (i.e. 2 s or less) and low signal to noise ratios.

The scope of this thesis is to revisit and improve old thermal-based interface technology and demonstrate its potential as a simple and cost-effective alternative to cryogenic modulation. The absence of moving parts and cryogenic consumables extend the applications of GC×GC instrumentation to on-site analysis, the most representative analysis of all. The following chapters entail the development of the modulator, its evaluation and comparison to cryogenic counterparts, and its applicability to the field analysis and monitoring of organics ($PM_{2.5}$) in urban air.

1.4 References

[1] Górecki T, Harynuk J, Panić O (2004) J Sep Sci 27(5-6):359-379

[2] Panić O, Górecki T (2006) J Anal Bioanal Chem 386(4):1013-1023

[3] Górecki T, Panić O, Oldridge N (2006) J Liquid Chromatogr & Rel Tech 29(7-8):1077-1104

[4] Giddings JC (1984) Anal Chem 56(12):1258A-1270A

[5] Bertsch W (1990) Multidimensional Gas Chromatography, in: Cortes HJ, Multidimensional Chromatography – Techniques and Applications, Marcel Dekker Inc., New York and Basel.

[6] de Geus HJ, Wester PG, Schelvis A, de Boer J, Brinkman UATh (2000) J Environ Monit 2:503-511

[7] Mrowetz SHJ (1983) J Chromatogr A 279:173-187

[8] Duinker JC, Schultz DE, Petrick G (1998) Mar Pollut Bull 19(1):19-25

[9] Storr-Hansen E (1991) Int J Environ Anal Chem 43(4):253-266

[10] Silvis LD, Kapila S, Yan Q, Elseewi AA (1994) J Chromatogr A 688:221-230

[11] Schurig V, Reich S (1998) Chirality 10(5):425-429

[12] Phillips JB, Liu Z (1991) J Chromatogr Sci 29(6):227-231

[13] Skoog DA, Holler FJ, Nieman TA (1998) Principles of Instrumental Analysis 5th Ed, Brooks/Cole, Thomson Learning , Australia, Canada, Mexico, Spain, UK, US

[14] Ryan D, Morrison P, Marriott P (2005) J Chromatogr A 1071:1585-1594

[15] Murphy R, Schure M, Foley J (1998) Anal Chem 70:1585-1594

[16] Blumberg LM (2003) J Chromatogr A 985(1-2):29-38

[17] Ong RCY, Marriott PJ (2002) J Chromatogr Sci 40:276-291

[18] Lee AL, Bartle, KD, Lewis AC (2001) Anal Chem 73:1330-1335

[19] Górecki T, Harynuk J, Panić O (2003) Comprehensive Two-Dimensional Gas Chromatography, in: Namiesnik J, Chrzanowski W, Zmijewska P, New Horizons and Challenges in Environmental Analysis and Monitoring, Centre for Excellence in Environmental Analysis and Monitoring (CEEAM), Gdansk, Poland.

[20] Harynuk J, Górecki T, Campbell C (2002) LC-GC N America 20(9):876-892

[21] Dalluge J, Beens J, Brinkman UATh (2003) J Chromatogr A 1000:69-108

[22] Beens J, Boelens H, Tijssen R, Blomberg J (1998) J High Resol Chromatogr 21:47-54

[23] Schoenmakers PJ, Oomen JLMM, Blomberg J, Genuit W, van Velzen G (2000) J Chromatogr A 892:29-46

[24] Harynuk J, Górecki T, Zeeuw J (2005) J Chromatogr A 1071(1-2):21-27

[25] Beens J, Janssen HG, Adahchour M, Brinkman UATh (2005) J Chromatogr A 1086:141-150

[26] Marriott PJ, Haglund P, Ong RCY (2003) Clinica Chimica Acta 328(1-2):1-19

[27] Bordajandi L, Ramos L, Gonzalez M (2005) J Chromatogr A 1078(1-2):128-135

[28] Hua R, Wang J, Kong H, Lie J, Liu J, Lu X, Xu G (2004) J Sep Sci 27(9):691-698

[29] Wang FC, Robbins WK, Greaney MA (2004) J Sep Sci 27(5-6):468-472

[30] van Stee LLP, Beens J, Vreuls RJJ, Brinkman UATh (2003) J Chromatogr A 1019(1-2):89-99

[31] Phillips JB, Ledford EB (1996) Field Anal Chem Tech 1(1):23-29

[32] Phillips JB, Gaines RB, Blomberg J, van der Wielen FWM, Dimandja J-M, Green V, Granger J, Patterson D, Racovalis L, de Geus HJ, de Boer J, Haglund P, Lipsky J, Sinha V, Ledford EB Jr. (1999) J High Resol Chromatogr 22(1):3-10

[33] Harynuk J, Górecki T (2002) J Sep Sci 25(5-6):304-310

[34] Burger BV, Snyman T, Burger WJG, van Rooyen WF (2003) J Sep Sci 26:123-128

[35] Kinghorn RM, Marriott P (1998) J High Resol Chromatogr 25(5-6):304-310

[36] Harynuk J, Górecki T (2001) Pittcon, New Orleans, LA, March 5-9, Abs. 108

[37] Ledford Jr. EB, Billesbach C (2000) J High Resol Chromatogr 23(3):202-204

[38] Beens J, Adachour M, Vreuls RJJ, van Altena K, Brinkman UATh (2001) J Chromatogr A 919(1):127-132

[39] Ledford EB, Billesbach C (2002) J Pittcon, March 17-22, New Orleans, LA, Contr. #2262P

[40] Harynuk J, Górecki T (2003) J Chromatogr A 1019(1-2):53-63

[41] Sacks R, Libardoni M, Waite JH (2005) Anal Chem 77(9):2786-2794

[42] Libardoni M, Hasselbrink E, Huner Waite J, Sacks R (2006) J Sep Sci 29:1001-1008

[43] Bruckner CA, Prazen BJ, Synovec RE (1998) Anal Chem 70:2796-2804

[44] Seeley JV, Kramp F, Hicks CJ (2000) Anal Chem 72:4364-4352

[45] Bueno PA, Seeley JV (2004) J Chromatogr A 1027(1-2):3-10

[46] Micyus NJ, McCurry JD, Seeley JV (2005) J Chromatogr A 1086(1-2):115-121

[47] Kochman M, Gordin A, Alon T, Amirav A (2006) J Chromatogr A 1129:95-104

[48] Dagan S, Amirav A (1994) Int J Mass Spectrometr Ion Proc 133:187-195

[49] Beens J, Brinkman UATh (2005) Analyst 130(2):123-127

[50] Song D, Marriott P, Wynne P (2004) J Chromatogr A 1058(1-2):223-232

[51] Seeley JV, Micyus NJ, Bandurski SV, Seeley SK, McCurry JD (2007) Anal Chem 79:1840-1847

[52] Deans DR (1981) J Chromatogr 203:19-28

2 Experimental Procedures

The interface and all required supplies were constructed in-house from commercially available materials. The trapping capillaries were developed from MXT-1 15 cm × 0.28 mm × 3 μm / 1 μm Silcosteel® capillaries, as well as from 15 cm × 0.28 mm deactivated Silcosteel® guard tubing (Restek, Bellefonte, PA). All traps were mechanically flattened to an inner distance of 0.1 mm from wall to wall with a custom-designed flattening device, described in detail in chapter 3. The ends of the capillaries, however, were not flattened in order to facilitate the ferrule-based connection to the column train. Initially, a roller system, with a user-controlled distance between the rollers, was built by the University of Waterloo's Science & Technical Services (STS). The current and more efficient method for flattening the trapping capillaries (illustrated in Figure 3.3) is based on two parallels and shims. The 3/8" × 3/4" × 6" parallels were purchase locally (KBC Tools, Kitchener, ON) and their edges were smoothened with a stone grinder in the student machine shop. Two 0.005" stainless steel shims were cut into strips representative of the length of the flattened trapping capillary (ca. 15 cm × 1 cm). The dimensions of the flattened trap were determined by measuring the tubing thickness with a metric micrometer (Mitutoyo, Japan). Serving as the middle electrical contact, a short piece (~1 - 2 cm) of flattened sacrificial Silcosteel® capillary (Restek, Bellefonte, PA) was spot-welded at the midpoint of and perpendicular to the trapping capillary. The remaining two contacts were completed with alligator clips at the stainless steel connector nuts. Installation of the trap in the upper wall of the GC oven required drilling two holes

for securing the trapping capillary and one for installing the middle contact mount (illustrated in Figure 3.2 B). The mount was constructed in the STS student machine shop from an aluminum rod, ceramic stand-offs, a banana jack, and a machineable ceramic plate (ca. 1 cm × 3 cm). A detailed diagram of the mount is depicted in Figure 2.1. The mount was installed on the upper wall of the GC oven (black). The top portion was used to secure and connect the trap's middle electrical contact to the power supply via the banana jack. Inside the GC oven, a ceramic plate (gray) separated the electrical contacts on the two ends of the trap from each other and simultaneously relieved pressure from the middle contact. The latter was achieved by resting the stainless steel unions connecting the trap to the 1D and 2D columns on the ceramic plate, with the columns going through grooves machined in the plate.

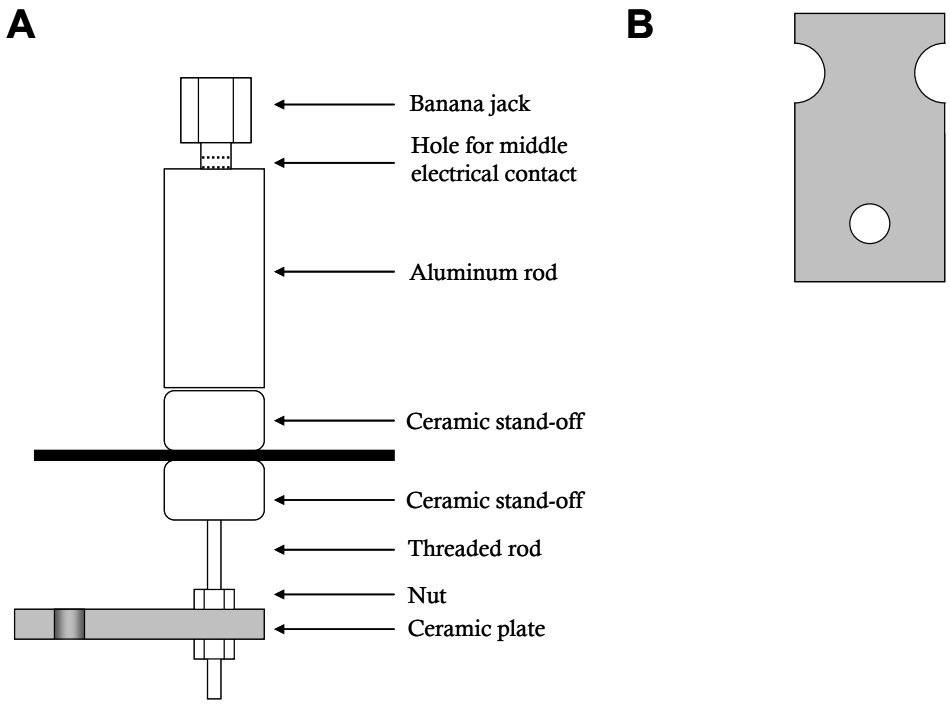

Figure 2.1. *Block diagram of the mount (A); top-down view of the machineable ceramic plate, showing the middle hole for the threaded rod and two grooves for the columns (B).*

Restrictor tubing was installed between the first dimension column and the trapping capillary. It consisted of a 6 cm segment of 0.1 mm ID deactivated fused silica capillary (Chromatographic Specialties, Brockville, ON). Individual components of the column train were connected with stainless steel Siltite miniunions (SGE, Austin, TX).

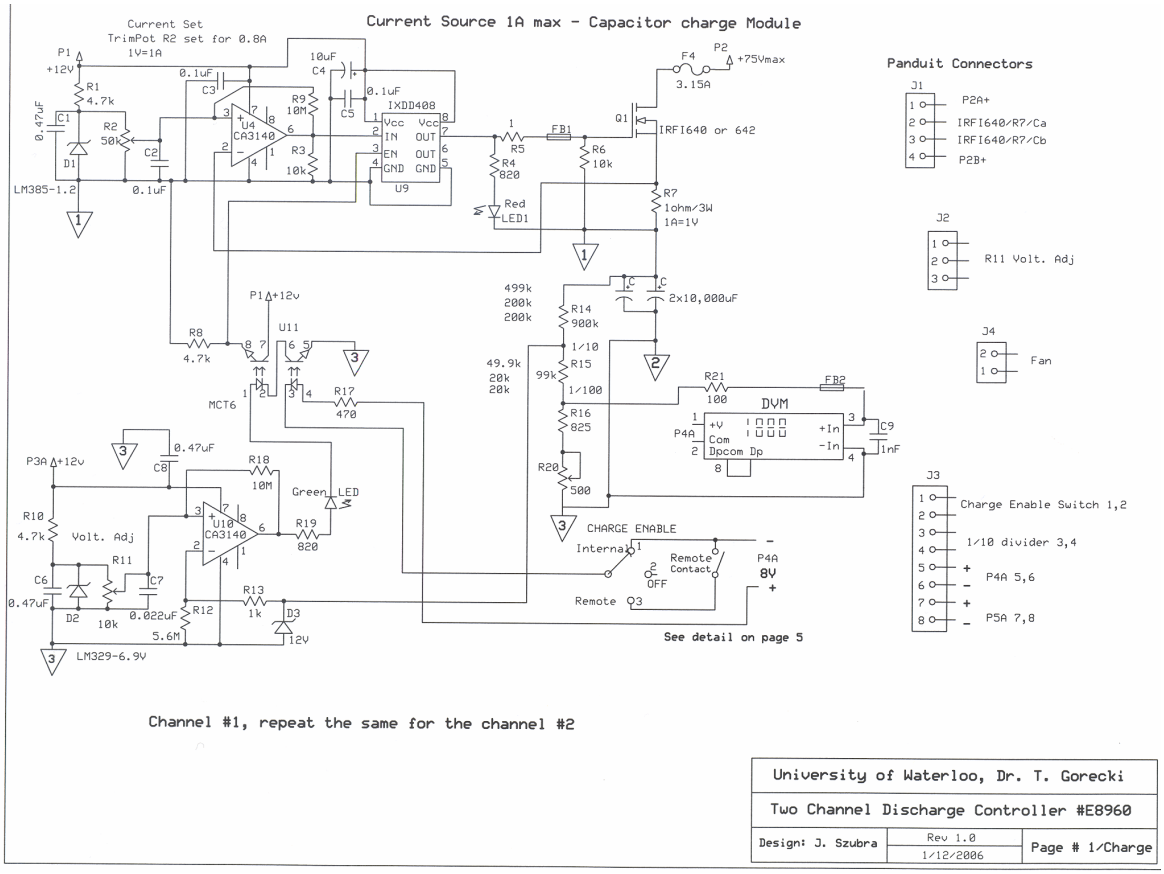

Figure 2.2. *Electronic diagram of the dual-channel capacitive discharge power supply, used for modulation by alternatively heating two segments of the trapping capillary (designed by STS).*

Resistive heating of the trapping capillaries was carried out with a dual-channel capacitive discharge power supply that was custom-designed and constructed by STS. The power supply was equipped with variable, user-controlled

discharge voltage and modulation period functions. The electronic diagram is provided in Figure 2.2. Calibration of the capacitive discharge power supply was carried out by recording the temperature generated across designated lengths of trapping capillary at various discharge voltages. Measurements were carried out using a 50 μm chromel/alumel K-type thermocouple (Omega, Laval, PQ) made by spot-welding the thermocouple wires one on top of the other onto the capillary. The signal was acquired with a PM 3365A 100 MHz digital oscilloscope (Phillips, Toronto, ON). Depending on the volatility of the compounds analyzed, the capacitive discharge power supply was operated to generate desorption temperatures between 275 ˚C and 325 ˚C. Additionally, the power supply was used to selectively remove stationary phase along the trapping capillary. This was achieved by subjecting selected segments of the trap to frequent discharge events (4 s apart) generating temperatures well in excess of 400 ˚C. The efficiency of this thermal degradation process is discussed in section 3.1.

Forced cooling of the trapping capillary was accomplished by utilizing commercially-available blowers. A Conair 1625 W hairdryer was purchased locally and used for the analysis of semi-volatile mixtures. Modulating volatile samples required the use of a dual nozzle adjustable spot cooler, also known as a Vortex tube (Exair Corporation, Cincinnati, OH). In both setups, the blower temperature was monitored during GC×GC analyses with a K-type thermocouple and model 8529-00 digital thermocouple thermometer (Cole-Parmer Instrument Company, Chicago, IL). The thermocouple junction was positioned ca. 1-2 mm from the nozzle of the blower.

The majority of the experiments were performed on a model 6890 gas chromatograph (Agilent Technologies, Mississauga, ON); some experiments were conducted with the Trace GC Ultra upgraded with 2D-GC modulator hardware (Thermo Electron Corporation, Milan, Italy). Both gas chromatographs were equipped with a split/splitless (S/SL) injector and were operated with hydrogen as the carrier gas, set at a constant flow of 1.2 mL/min. Data was acquired with FID at 100 Hz (Agilent) and at 120 Hz (Thermo). The 1st dimension column was a VF-5ms 30 m × 0.25 mm × 1 μm/0.5 μm (Varian, Canada), and the 2nd dimension column was a SolGel WAX 1.4 m/2.5 m × 0.25 mm × 0.25 μm (SGE Inc., Austin, TX). For testing of the injection band width, the second column was replaced with a 0.9 m × 0.25 mm uncoated fused silica capillary (Chromatographic Specialties, Brockville, ON). Manual injections of the samples and standards (1 μL) were carried out using hot needle technique. Chromatographic parameters and data collection were controlled with Agilent's Chemstation software and Thermo's ChromQuest software. Generation of GC×GC chromatograms required exporting the linear FID signals as comma delimited files (.csv) and processing them with software written in-house in Matlab (Mathworks, Natick, MA).

Evaluation of the interface was conducted with standard solutions containing *n*-hexane to *n*-decane (Sigma-Aldrich, St. Louis, MO) in CS_2 (EMD Chemicals Inc., Gibbstown, NJ) and *n*-octane to *n*-tridecane (Sigma-Aldrich, St. Louis, MO) in CS_2 (EMD Chemicals Inc., Gibbstown, NJ). The working volatility range of the interface was determined by analyzing a linear alkane standard consisting of *n*-octane to *n*-tetracontane in chloroform (AccuStandard Inc., New Haven, CT). The system's

suitability for analyzing complex samples was evaluated with petrochemical mixtures. Unleaded 87 octane gasoline and diesel fuel were obtained from a local gas station. Kerosene was purchased from a local hardware store. Machining spindle oil (Castor) was obtained from Linamar Corporation, Guelph, ON. Polychlorinated biphenyls (PCBs) were analyzed as technical mixtures Arochlor 1260, Arochlor 1254, 1:1 mixture of Arochlor 1260/1254, and Arochlor 1260 in transformer oil (Supelco, Bellefonte, PA). The pesticide toxaphene was obtained from Supelco, Bellefonte, PA. Undiluted essential oils of rosemary (*Rosmarius officinalis*), sage (*Salvia officinalis*) and neroli (*Citrus aurantium*) were purchased at a local health food store. 2D-TAG was initially tested with a 37 component fatty acid methyl ester (FAME) standard mixture (Sigma-Aldrich, St. Louis, MO) and the EPA method 8270 working standard (Cerillian Corporation, Round Rock, TX). Ambient air was collected for ca. 2 hours and was analyzed with 2D-TAG on January 27th, 2006 in Berkeley, CA. Experimental conditions specific to each sample are summarized in Table 2.1.

Table 2.1. *Summary of the experimental conditions for the different analyses; desorption temperatures between 275 and 325 ˚ C and modulation period of 6 s.*

Sample	Oven Temperature Program * [˚C(minutes)]	Blower Temperature (˚C)	Injector/Detector Temperature (˚C)	Trap Stationary Phase Film Thickness (μm)
n-C_6 – *n*-C_{10}	35(3)→240	- 8	250 / 250	1
n-C_8 – *n*-C_{13}	70→240	25	250 / 250	1
n-C_8 – *n*-C_{40}	35(3)→280 (120)→290(10)	110	250 / 280	1/deactivated
Gasoline	35(3)→260	- 12	250 / 250	3
Kerosene	35(3)→260(30)	- 8	250 / 280	1
Diesel	70→260(3)	25	250 / 280	1
Spindle oil	100→270(30)	25	280 / 280	1
Aroclor 1260	125→270(25) →280(15)	110	250 / 250	1
Aroclor 1254	115→270(25) →280	110	250 / 250	1
Aroclor 1260/1254	125→260(45) →270(35)→280	110	250 / 250	1
Aroclor 1260 in transformer oil	125→260(45) →270(35)→280	110	250 / 250	1
Toxaphene	100→260(30) →270(15)→280	110	250 / 250	1
Neroli oil	70(3)→260(40)→ 280(10)	25	250 / 250	1
Sage oil	70(3)→260(30)	- 9	250 / 250	1
Rosemary oil	70(3)→260(10)	- 10	250 / 250	1
Sandalwood oil	70(3)→260(40)→ 280(10)	25	250 / 250	1
Fatty acid methyl esters (FAMEs)	35(3)→260(30)	25	250/250	3
EPA method 8270	35(3)→260(30)	25	250/250	3
Air	35(3)→260(30)	25	250/250	3

* Temperature ramp was 3 ˚C/min.

3 Development of the Interface

This project arose from a collaborative effort towards the development and application of GC×GC instrumentation for field analysis and monitoring of semi-volatile organic compounds in urban air particulate matter ($PM_{2.5}$), conducted by Dr. Allen Goldstein at the University of California in Berkeley. Commercially available cryogenic GC×GC systems are not suitable for this purpose because consumables such as liquid N_2 and/or CO_2 make them impractical for field operation and non-optimal for the analysis of semi-volatile mixtures. Examples of modulator designs capable of achieving this goal are the early heater-based modulators and the latest valve-based interfaces. It is important to note that while the latter provide a relatively simple and cheap approach to performing GC×GC separations, they do not offer the same increase in separation power and sensitivity as thermal interfaces. This thesis documents the design and development of a simple heater-based modulator, operating without moving parts and cryogenic consumables.

Heater-based interfaces are no longer in use because they were initially labeled as inferior to cryogenic modulators (e.g. LMCS [1]). Lee et al. reported that while heater-based interfaces relying on restive heating of thick-film aluminum and/or stainless steel capillaries for modulation provided proof of concept, they were not optimal for GC×GC separations. More specifically, in the above study such modulators generated broad injection bands in the second dimension, failed to efficiently trap volatile compounds, and lacked robustness.

Early research in Dr. Górecki's laboratory yielded promising results when Silcosteel® capillaries were used for modulation [2]. Injection pulses presented to the second dimension column were dramatically narrower when the internal volume of the trapping capillary was decreased. Additionally, band broadening associated with gas expansion in a tube (in this case the Silcosteel® trapping capillary) upon heating was minimized with the installation of a short piece of small ID uncoated fused silica tubing between the first column and the trap. In this configuration, the short piece of tubing acted as a restrictor upstream of the trapping capillary.

The proposed GC×GC interface is depicted in Figure 3.1 A. Briefly, the modulator consists of a short piece of restrictor tubing, a flattened Silcosteel® trapping capillary, a cooling blower, and a custom-designed capacitive discharge power supply. A more detailed block diagram of the trapping capillary illustrates that the trap is mechanically flattened to achieve an inner spacing of ~ 100 μm from wall to wall (Figure 3.1 B). Dual-stage thermal modulation is carried out in the following manner: analytes eluting from the first dimension column enter the trapping capillary, whose lower temperature and thick-film promote partitioning into the non-polar stationary phase. This accomplishes analyte trapping and focusing. Re-mobilization of the analytes in the first segment of the trap is achieved by briefly passing electric current from the power supply through segment 1 of the Silcosteel® capillary (Figure 3.1 B). Upon reaching the second segment of the capillary, the desorbed analytes become re-trapped and focused once again. Simultaneously, the first segment of the trap cools down to prevent analyte breakthrough, while resistive heating of the second segment (segment 2 in Figure 3.1 B) injects a narrow band of

the refocused analytes onto the second column. This process is repeated throughout the entire GC×GC analysis.

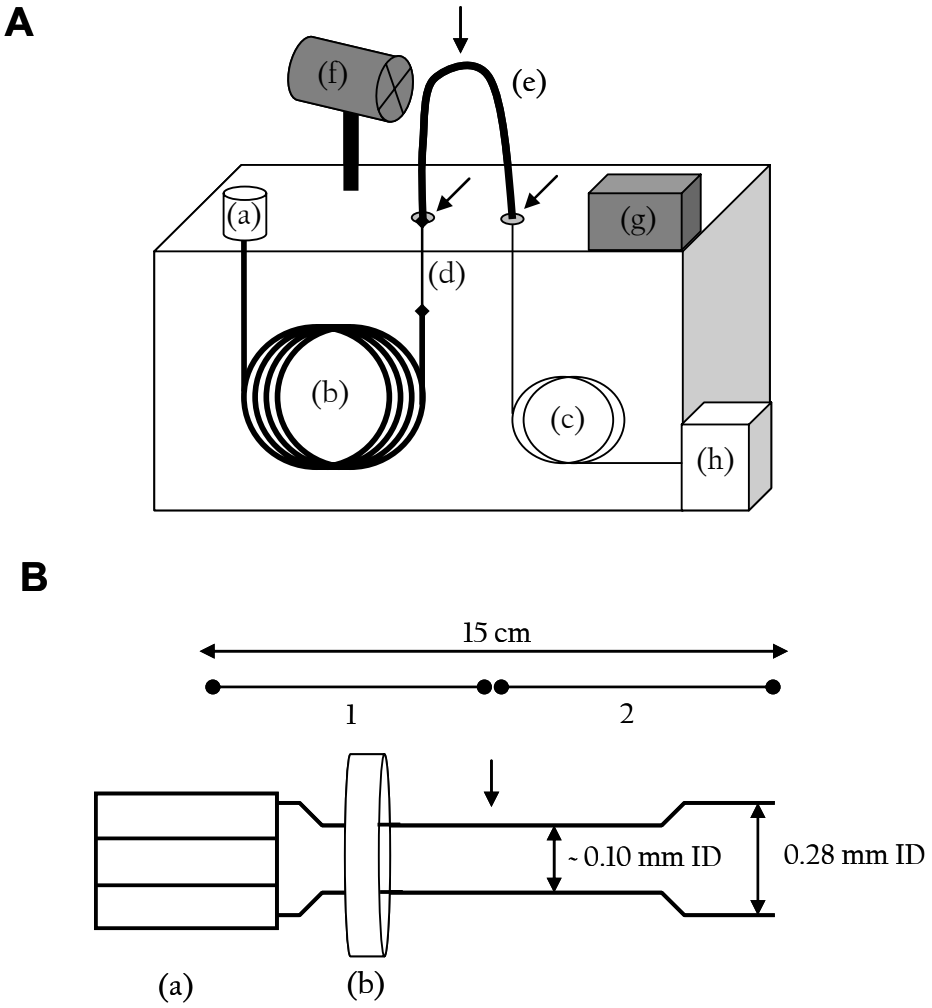

Figure 3.1. *The proposed GC×GC system. (A) A block diagram of the system, including (a) injector, (b) 1D and (c) 2D columns, (d) restrictor, (e) flattened trap with electrical contact at 3 points (arrows), (f) cooling blower, (g) power supply and (h) FID detector. (B) Enlarged sketch of the trapping capillary. The components shown on the left side, stainless steel mini-union (a) and silicone septum (b), are present on both sides of the trap. Segments 1 and 2 represent the two zones where resistive heating by the power supply occurs alternatively. The arrow points to the location of the middle electrical contact, while the 2 outside contacts are on the stainless steel nuts. The measurements of the distance between the walls are provided for both the flattened and the non-flattened parts of the trapping capillary.*

The following sections illustrate that by revisiting old interface technology and improving it with unique innovations, it was possible to develop a simple and cost-effective heater-based modulator that performs on-par with some cryogenic counterparts. In addition to offering the same advantages as any other thermal GC×GC system (increased resolution, sensitivity, and structured chromatograms), the proposed modulator represents a pioneering step towards the development of GC×GC instrumentation for field analysis and monitoring applications. A prototype of the modulator is already in use at the Department of Environmental Science, Policy and Management at UC Berkeley (CA). Dr. Goldstein integrated this modulator into the direct thermal desorption aerosol GC (TAG) system, a field instrument developed in his laboratory [3]. The GC×GC (2D-TAG) system will provide much more detailed information on urban air aerosols (see section 4) [4].

3.1 Trapping Capillary

Successful operation of heater-based modulators utilizing resistive heating for analyte desorption requires thin-walled, electrically conductive trapping capillaries coated inside with an appropriate stationary phase. The commercially available product that initially satisfied these requirements was a 0.28 mm ID Silcosteel® capillary coated with 3 μm of polydimethylsiloxane (PDMS) stationary phase. The length of trap was arbitrarily set at 15 cm. Previous experiments in Dr. Górecki's laboratory indicated that 0.53 mm ID Silcosteel® tubing coated with films thicker than 3 μm required long cooling times, making modulation periods of 3 - 6 s unachievable.

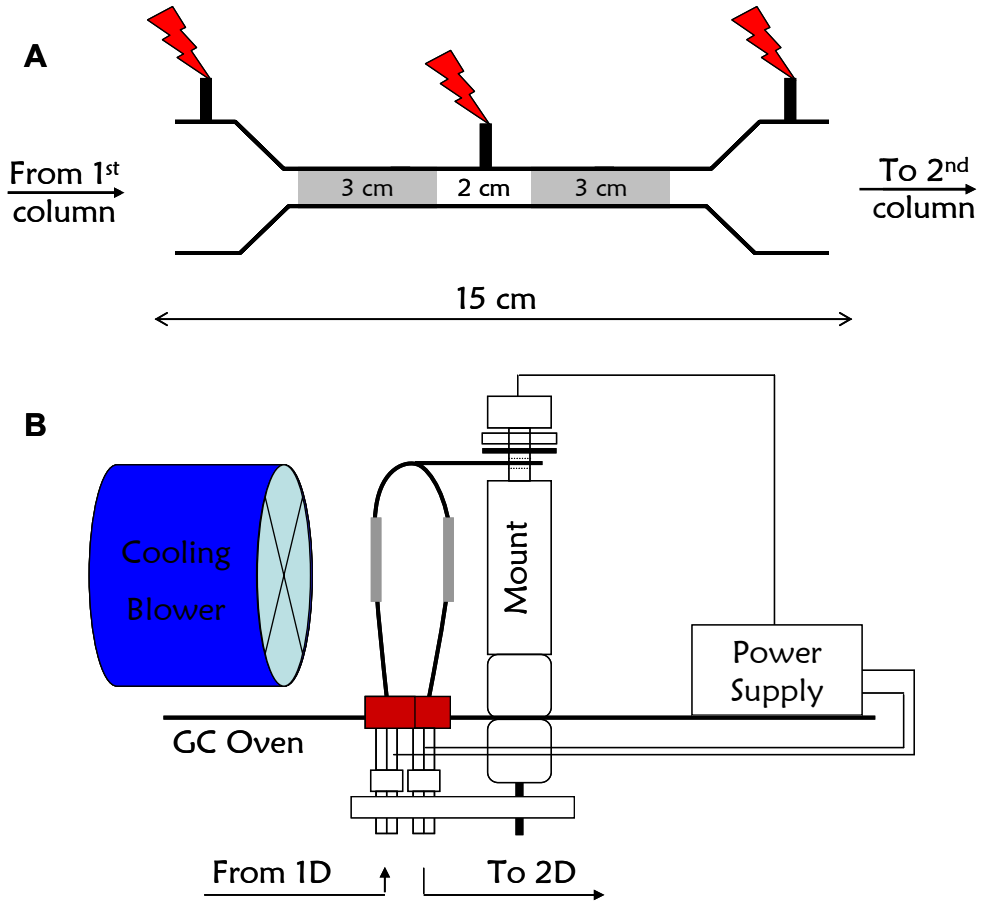

Figure 3.2. *Schematic diagrams of the trapping capillary. (A) The flattened trap with two trapping zones (gray). Electrical contacts (red) at 3 points ensure dual-stage modulation via resistive heating. (B) The trap installed on top of a GC oven and secured in place with GC septa (red) pushed into holes drilled in the oven top wall. The cooling blower was in close vicinity of the trapping capillary (~ 1 - 3 cm) and was continuously operated during analysis. Two electrical contacts were located at the stainless steel unions inside the oven, while the middle contact was provided by the middle mount. This mount simultaneously supported the two connectors inside the oven and relieved pressure from the spot-welded middle contact (details can be found in section 2).*

The trapping capillary and its installation on a gas chromatograph are depicted in Figure 3.2. The two inventions that were essential to the success of the current project are emphasized in Figure 3.2 A. They included the flattening of the trapping capillary and the selective removal of the stationary phase within this capillary. A restrictor between the first dimension column and the trap was installed

because it was reported to significantly enhance the performance of resistively heated modulators utilizing stainless steel capillaries [2].

The Silcosteel® trapping capillaries were initially flattened with a custom-designed roller system. This approach has been abandoned as it was laborious and highly irreproducible. Specifically, it was difficult to precisely achieve and maintain the desired ID, which led to non-uniform "flatness" along the tubing. The geometrical differences between individual traps were considered a potential source of irreproducibility. Nevertheless, trap prototypes made with the roller apparatus enabled proof of concept studies, which indicated that minimizing the wall to wall distance played a significant role in the narrowing of the injection bands introduced to the second dimension column (see Table 3.1). It is interesting to note that peak widths observed with non-flattened trapping capillaries were in close agreement with those reported in the study that originally classified such interfaces as inferior [1].

Other modulator prototypes were constructed and tested during the initial stages of this research. For example, a reduction of the trapping zone length from 3 cm to 1.5 cm, in an effort to enhance analyte focusing and generate narrower injection bands, proved relatively inconsequential. Another approach involved reducing the wall-to-wall distance at the midpoint of the flattened trapping capillary to ~ 70 μm. Theoretically, the pinched middle should act as a restriction to upstream gas flow during desorption in the second segment of the trap; however, no additional reduction in 2D peak widths was observed. In the final prototype, the lengths of the interface and the trapping zones were cut by half to decrease the amount of gas that would expand during the desorption events. This approach provided no significant

improvement compared to the original interface. Consequently, the reduction of the trap's internal volume by flattening the capillary proved to be the most significant factor contributing to the reduction of the second dimension peak widths.

Table 3.1. *Evaluation of several interface prototypes based on coated Silcosteel tubing with two trapping zones as in Figure 3.2 A.*

Description of Modulator Prototype	**2D Peak Width at Half Height (ms) ***
Flattened (as in Figure 3.2 A)	~ 120
Non-flattened	~ 350
Shorter trapping zones (1.5 cm)	~ 150
Pinched middle (~ 70 μm ID)	~ 150
Shorter trap length (7.5 cm)	~ 120

* All measurements of peak widths in the second dimension included band broadening effects in the secondary column.

The difficulties encountered during manufacturing of the traps with the roller system were alleviated by developing a more efficient method for flattening the trapping capillaries (Figure 3.3). First, the tubing was placed between two thin stainless steel sheets (0.005 " shims), each 15 cm in length (Figure 3.3 a). Masking tape was used to hold the capillary in place (Figure 3.3 b). Two 15 cm steel blocks, or parallels, with smoothened edges were placed on both sides of the trap, shims and tape, and were then inserted in this configuration into a vice (Figures 3.3 a and b). The force applied by turning the vice handle by ~90˚ flattened the tubing to the desired wall-to-wall distance, consistently ensured by the shims. The smoothened edges of the parallels prevented cracking of the tubing at the transition between the flattened and non-flattened sections of the trap. This procedure was relatively quick and easy; most importantly, it guaranteed ID uniformity throughout the entire trapping capillary and provided reproducibility between individual modulators. The

latter was chromatographically confirmed as the second dimension retention times between any two trapping capillaries did not differ by more than 15 ms. Presently, all trapping capillaries are flattened by the method illustrated in Figure 3.3.

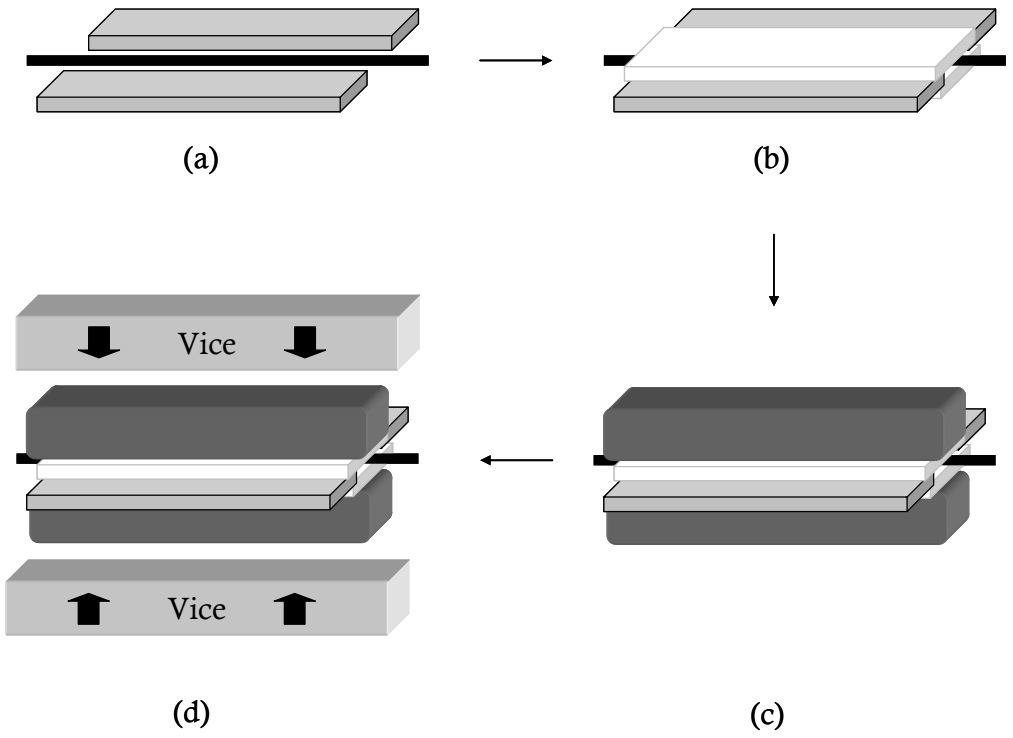

Figure 3.3. *Flattening of the trapping capillaries. (a) The tubing (black) was placed between two shims (gray) and was secured in place (b) with masking tape (white). (c) Two parallels were placed on both sides and inserted into a vice (d). The pressure applied by the vice ensured uniform and precise flattening of the trap along the entire 15 cm length.*

The second invention that caused a dramatic improvement of previously reported results with resistively heated thermal modulators was the selective removal of the stationary phase along the trapping capillary. Understanding the intent behind this invention requires a closer examination of Figure 3.2 B and the principles of first column effluent modulation. All heater-based interfaces utilizing resistive heating for

analyte desorption in the trapping capillary contain at least three electrical contacts to accomplish dual- or multi-stage modulation. These three contacts, in addition to the two GC septa (Figure 3.2 B), are extraneous masses in contact with the trapping capillary and consequently act as thermal sinks during desorption. The cold spots that they create are detrimental to the GC×GC separation because they lead to additional retention (at lower temperatures) within the trapping capillary, which subsequently causes peak broadening in the first dimension and tailing peaks in the second dimension. Figure 3.4 A illustrates that modulation of an *n*-alkane standard with a flattened trapping capillary coated with the stationary phase along its entire length leads to first dimension peak broadening that becomes more pronounced with decreasing volatility of the analytes. In retrospect, Phillips' first modulator [5] was soon replaced with the rotating heater interface [6,7] partially in an effort to eliminate cold spots caused by electrical contacts on the trapping capillary.

Band broadening associated with cold spots was observed very early in this research. In the initial modulator prototypes, an alligator clip was used as the middle electrical contact. This relatively bulky connection proved to be a significant thermal sink, giving rise to exceptionally broad peaks in the first dimension (Figure 3.4 A). An experiment designed to test this hypothesis illustrated that the broadening could be eliminated by the application of hot air (hairdryer set at ~ 110 ˚C during modulation) to warm the middle electrical contact, as illustrated in Figure 3.4 B.

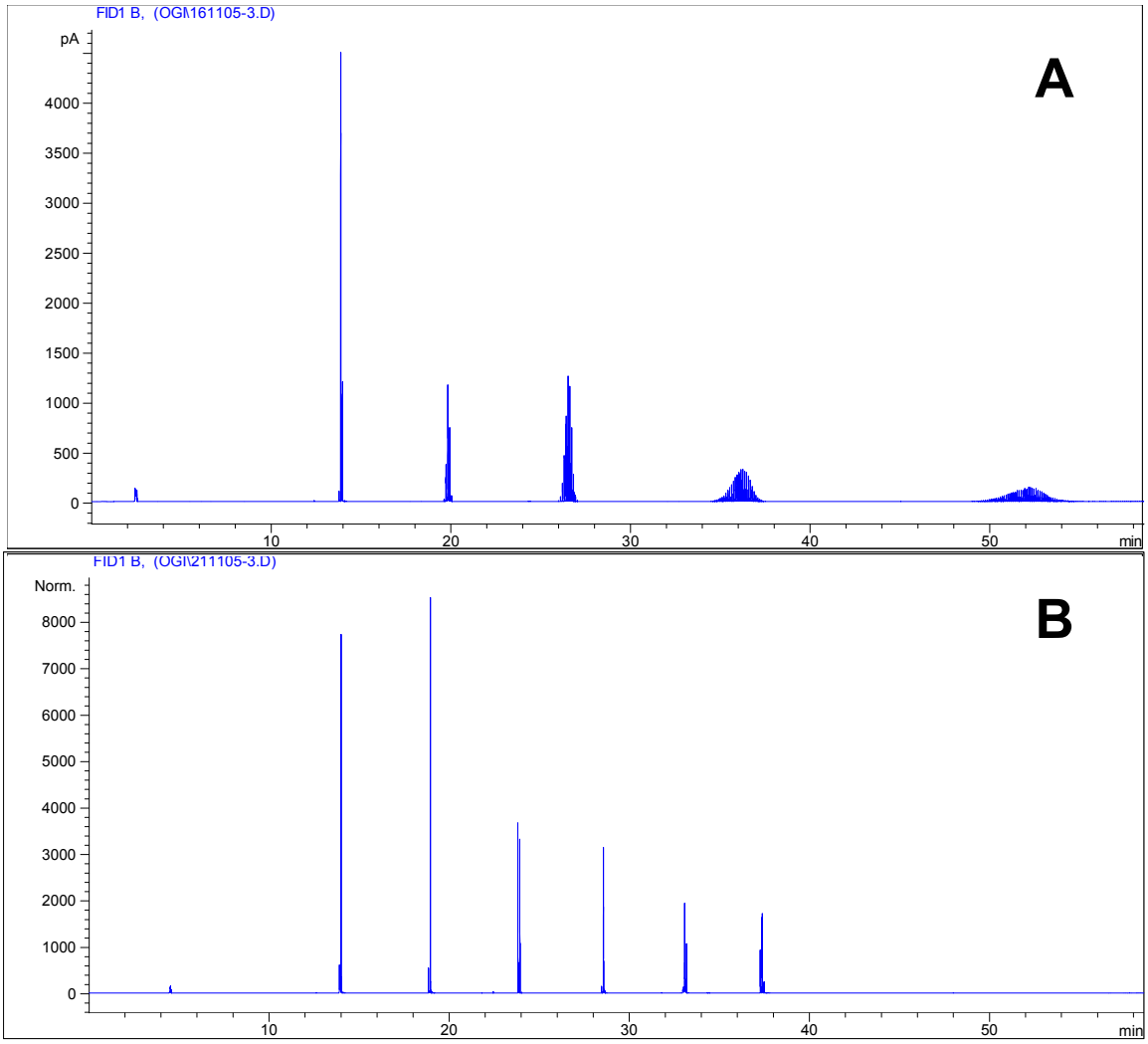

Figure 3.4. *The detrimental effect of cold spots on GC×GC separation of an n-alkane standard (C_8 to C_{13}) generated with resistively heated modulators. (A) Raw GC×GC chromatogram obtained with a flattened trapping capillary equipped with an alligator clip as the middle electrical contact. Band broadening worsened with increasing boiling point of the n-alkanes. (B) Application of hot air from a hairdryer during modulation of the same n-alkane sample eliminated the cold spot and the associated band broadening. The differences in retention times between the two chromatograms are due to additional retention at cold spots.*

Heating the middle electrical contact in order to eliminate cold spots was far from an ideal or a long-term solution. In fact, considering the relationship between the degree of band broadening and analyte volatility (Figure 3.4 A), it became obvious that an interface designed for the analysis of semi-volatile compounds

required a middle contact with the lowest possible thermal mass. A short piece of sacrificial Silcosteel® tubing, spot-welded to the midpoint of the trapping capillary, was used for this purpose (see Chapter 2). The introduction of the spot-welded middle contact led to the construction of the middle mount, described in detail in the experimental section. Ultimately, minimization of the effect of the cold spots in the proposed interface was achieved by destroying the stationary phase around all potential thermal sinks. The removal of the PDMS film around the three electrical contacts and the GC septa generated two trapping zones (areas with intact stationary phase), as illustrated in Figure 3.2. In addition to permitting the analysis of less volatile analytes, the selective removal of the stationary phase had a significant positive impact on peak width and symmetry in the second dimension (Figure 3.5).

Eliminating stationary phase in designated areas of the trapping capillary was accomplished by thermally degrading the PDMS coating. The capacitive discharge power supply was set at a discharge voltage that would resistively heat a segment of the trapping column above the manufacturer-recommended upper temperature limit (i.e. 350 ˚C). In this case, frequently repeated heating events (4 s apart) applied to a particular segment of the trapping capillary caused the tubing to glow red. As the temperature far exceeded 400 ˚C in these zones, most of the stationary phase was assumed to be destroyed. Initially, the number of discharge events for this purpose was arbitrarily set at 10 – 13. This was later demonstrated to be inefficient and incomplete. For example, when 13 discharge events were used to destroy stationary phase in the trapping capillary, modulated *n*-alkane peaks in the GC×GC chromatogram exhibited tailing in the second dimension (Figure 3.5 A).

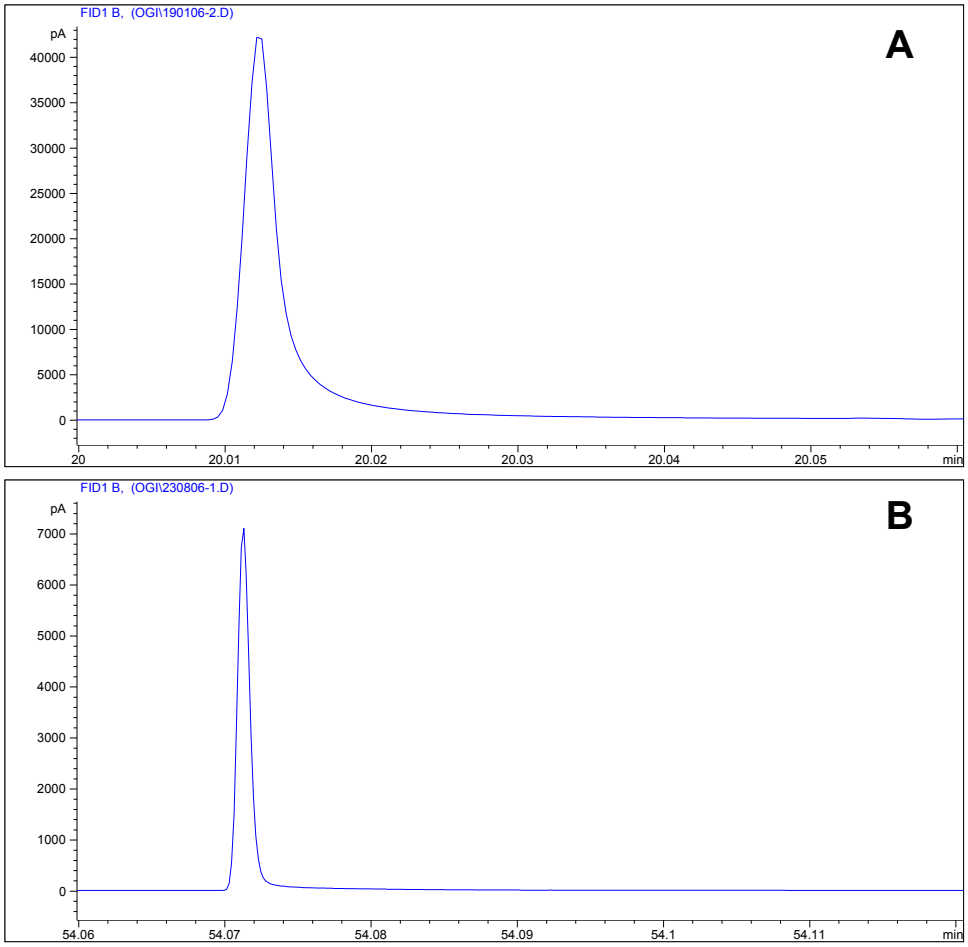

Figure 3.5. *The effect of the efficiency of stationary phase removal on GC×GC separation. (A) Raw GC×GC chromatogram illustrating one slice of an n-alkane peak generated with a flattened trapping capillary subject to removal of stationary phase with 13 consecutive discharge events. Tailing was evident and the peak width at half height was ~120 ms. (B) The same slice was 60 ms wide at half height when the selective removal of the stationary phase in the trap was achieved with 30 consecutive discharges. Elimination of tailing was due to the elimination of cold trapping spots in the interface, making analyte desorption a more efficient process.*

Tailing peaks in chromatography are undesirable and hinder analyte quantification. Following this, a series of experiments were carried out to determine the number of discharge events required to ensure removal of the stationary phase in the trap that would produce results comparable to an interface constructed from uncoated deactivated Silcosteel® capillaries. It was determined that this was achieved when

the number of consecutive discharge events was at least 30. Figure 3.5 B illustrates that flattened trapping capillaries in which the PDMS film was selectively removed with the aforementioned procedure generated GC×GC chromatograms with symmetrical peaks. In addition, the procedure had a profound impact on 2D peak widths. Previously recorded peak widths in the second dimensions of ~120 ms (Figure 3.5 A) were decreased to ~60 ms at half height when the selective removal of the stationary phase was complete (Figure 3.5 B).

The significance of the upstream restrictor was examined only after a satisfactory interface prototype was developed. The use of restriction tubing was originally reported to play a significant role in enhancing peak symmetry and narrowing injection band widths presented to the second dimension [2]. While the resistively heated modulators designed by Harynuk and Górecki shared some similarities with the one presented in this thesis, the trapping capillaries they utilized had considerably larger inner diameter (0.53 mm). With the proposed interface, GC×GC separations conducted without the restrictor did not differ from those that incorporated this component in the column train. One plausible explanation for this observation is that the flattened trapping capillary (0.1 mm ID) minimized the volume of the carrier gas present in the trap, and thereby reduced band broadening associated with gas expansion during desorption. Since the trapping capillary itself posed a significant resistance to gas flow, efforts towards implementing restrictor tubing with smaller inner diameter (e.g. 50 μm) were abandoned for practical reasons, as that would require the use of excessive inlet pressures. In conclusion, the restrictor was found not to be a necessary instrumental component.

3.2 Capacitive Discharge Power Supply

The Science Technical Services (STS) constructed a custom-designed capacitive discharge power supply suitable for the type of modulation required. The function of this device is to periodically and alternately heat two segments of a Silcosteel® trapping capillary, making dual-stage modulation possible (Figure 3.1 B). The power supply functions by discharging one capacitor through one channel, causing resistive heating of one trapping capillary segment (segment 1 in Figure 3.1 B); subsequently, discharging the second capacitor through another channel resistively heats the second segment of the trap (segment 2 in Figure 3.1 B). The power supply featured adjustable modulation period and discharge voltage (0–60 V) that allowed for flexibility during developmental stages of the research.

Researchers operating custom-made GC×GC systems with in-house written data processing software can face difficulty when converting the linear data to 2D representation. In theory, generating a GC×GC plot requires slicing the original chromatogram according to the modulation period. Many home-built systems, however, measure modulation periods and chromatographic retention times with two different clocks, one in the interface and another one in the GC electronics. What is defined as 3.000 s by the interface might for example be recorded by the GC detector as 3.001 s. Since this time difference is cumulative during the entire GC×GC analysis, entire 2D "slices" might be misplaced in the final chromatogram. This implies that re-injection times into the second column, instead of the modulation period, should be used for generating GC×GC plots. Accordingly, some researchers record a timestamp file along the original chromatogram as a means of

obtaining individual re-injection times to properly "slice" the raw GC×GC chromatogram. The power supply used in this research utilized the FID clock signal for its timing purposes, eliminating the possible time base discrepancies between the modulator and the detector electronics. Therefore, the need for timestamps was eliminated and the overall operation of the system was simplified.

Calibration of the power supply involved the determination of discharge voltages required to heat segments of the 0.28 mm ID trapping capillary with a wall thickness of 0.13 mm to the desired temperatures. Temperature measurements were obtained from oscilloscope readings of the signal generated by thin wire thermocouples spot-welded onto the trapping capillaries (experimental details can be found in Section 2). A brief summary of these results is illustrated in Table 3.2. It is important to note that while heating of the trap to a higher temperature led to efficient desorption of the analytes, it simultaneously contributed to longer cooling times and led to stationary phase bleed. The optimum desorption temperature range, resulting in narrow 2D injection bands and minimal bleed from the trap, was experimentally determined to be 275 to 325 °C.

Table 3.2. *Calibration of the power supply with a 0.28 mm ID Silcosteel® trapping capillary (0.13 mm wall thickness) with no forced cooling.*

Length of Trapping Capillary (cm)	Discharge Voltage (V)	Recorded Temperature (°C)	Recorded cooling time (s)
7	33.3	225	8.5
7	34.2	250	9
7	36.6	275	10
7	37.3	300	12
7	39.4	325	13.5
7	42.0	365	15

3.3 Cooling Blower

Efficient modulation with heater-based interfaces depends on rapid heating and cooling of the trapping capillary [2,8]. The capacitive discharge power supply ensured prompt and reproducible heating of the interface; however, the trap was characterized by long cooling times (Table 3.2). For example, when heated to 325 ˚C, the trapping capillary required 13.5 s to cool. At these conditions, analyte breakthrough could only be prevented by applying modulation periods longer than 13 s, an approach that is highly impractical. Alternatively, more acceptable modulation periods (~ 6 s) could be achieved if the cooling rate of the trapping capillary was increased with the aid of a blower.

The importance of the cooling blower and its effect on the efficiency of modulation are depicted in Figure 3.6. Without forced cooling, alternatively heating the two segments of the trapping capillary to 275 ˚C did not ensure successful modulation of an *n*-alkane standard. Even at a modulation period of 9 s, analyte breakthrough was observed as a raised baseline between two slices in the unprocessed GC×GC chromatogram. The breakthrough of *n*-undecane (C_{11}) is marked in Figure 3.6 A. When air from the laboratory compressed air line was used to rapidly cool the trapping capillary during modulation of the same *n*-alkane standard, analyte breakthrough was completely eliminated. The raw GC×GC chromatogram in Figure 3.6 B confirms this as *n*-undecane (in the same *n*-alkane standard) was properly trapped with a modulation period of 6 s. The incorporation of a cooling blower therefore eliminated analyte breakthrough and simultaneously permitted the use of shorter modulation periods.

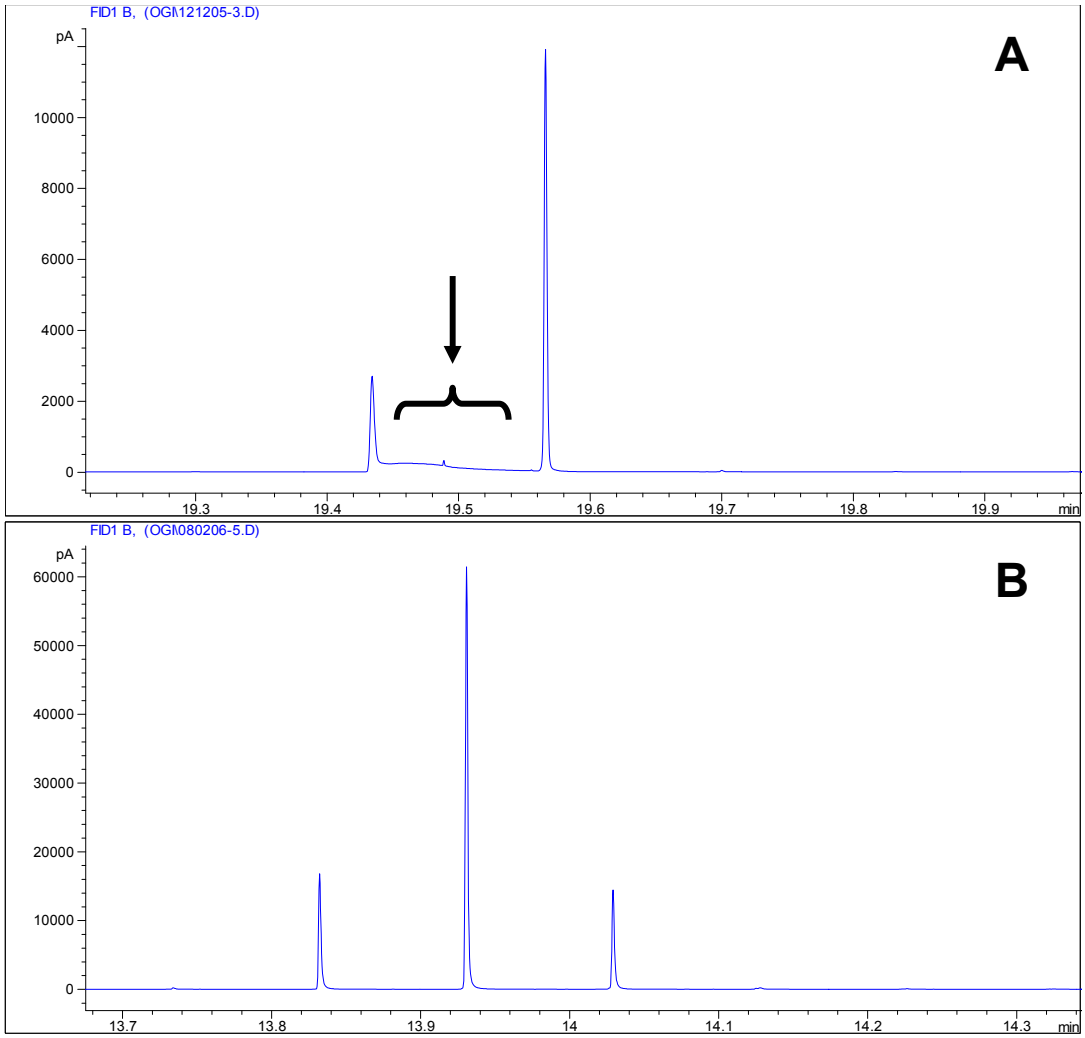

Figure 3.6. *The effect of the cooling blower on modulation efficiency. (A) Part of a raw GC×GC chromatogram, illustrating inefficient modulation of n-undecane with a modulation period of 9 s. Analyte breakthrough (arrow) was observed between the two injection bands. (B) In a similar analysis of an n-alkane standard with the application of forced cooling (compressed air from the laboratory compressed air line), n-undecane could be efficiently trapped even with a modulation period of 6 s.*

Initial solutions for forced cooling included a compressed air line and various types of personal computer central processing unit (CPU) cooling fans. However, anticipated routine use in conjunction with the field equipment at the Berkeley laboratory suggested the implementation of a readily available electric blower – a

hairdryer. The temperatures produced by the hairdryer when permanently set on the cool and hot functions were measured as 25 ˚C and 110 ˚C, respectively. The later stages of this research focused on the analysis of more volatile mixtures, carried out independently of the work conducted in Berkeley (see section 3.4). For this purpose, a commercially available blower based on vortex tube technology was utilized. Discovered by the French physicist Georges Ranque, a vortex tube requires a continuous supply of compressed air, a portion of which is converted to cold air and expelled at one end of the tube, while at the other end the remaining fraction exits as hot air [9]. Figure 3.7 briefly explains how a vortex tube works. The temperatures generated by the vortex tube can be controlled by the user by changing the amount of air that is converted to the hot fraction via a rotary dial. The particular model of the cooler utilized in the research could generate cool air in the range from -20 ˚C to +20 ˚C when supplied with room temperature compressed air.

Figure 3.7. *Design of a Vortex cooler. Pressurized air (vertical arrow) enters the tube at a right angle. Air molecules with high kinetic energy exit the back of the tube as hot air (maroon arrows); air molecules with lower energy (blue) travel through the centre of the tube and are ejected through the nozzle as a stream of cool air [10].*

3.4 Evaluation of the Interface

Evaluation of interface technology is frequently carried out with simple standard mixtures. For this purpose, a set of *n*-alkanes (C_8 – C_{13} in CS_2) was used to test the interface performance. Injection bands presented to the second column, peak widths in the second dimension, overall peak shape, and gains in sensitivity were all of primary importance. It should be noted that interface evaluation experiments required the optimization of all parameters discussed in the preceding sections. In an effort to successfully modulate semi-volatile compounds, initial analyses of standard mixtures were conducted with traps coated with 3 μm films of PDMS.

The quality of modulation is most accurately characterized by the width of the injection bands presented to the second dimension. In an experiment with a short transfer line (uncoated deactivated fused silica tubing) in place of the second column, the proposed interface produced injection bands as narrow as 60 ms at half height (Table 3.3). It has been observed that on average, the injection bands generated by the trapping capillary were on the order of 70 – 80 ms at half height. Following the installation of an actual 2D column, peak broadening in the second dimension accounted for the increase in peak widths to ~ 120 ms. Nevertheless, the results presented in Table 3.3 are astonishing, considering that Lewis et al. previously reported peak widths in excess of 350 ms for home made heater-based interfaces utilizing resistively heated stainless steel capillaries [1]. Furthermore, a comparison of peak widths at half height generated with our interface to those reported by Marriott et al. using LMCS suggests comparable performance to at least some cryogenic modulators [11,12].

Table 3.3. *Comparison of 2D peak widths generated with the interface developed and other selected modulators.*

Interface Description	**2D peak width at half height ($w_{1/2}^{2D}$) [ms]**
Proposed interface (injection band widths – no 2D column)	60
Proposed interface (peak widths with a 2D column)	120
Lee et al. (i.e. evaluation of stainless steel modulators) [1]	350
LMCS (i.e. original cryogenic modulator) [11,12]	100

In addition to evaluating the quality of the interface, the system's overall ability to perform a GC×GC separation was tested. For this purpose, diesel fuel was analyzed (Figure 3.8). The 1D-GC analysis of diesel exhibits a hump in the baseline that consists of many unresolved compounds (Figure 3.8 A). The raw GC×GC chromatogram is characterized by narrower and taller peaks, due to the modulator's focusing effects (Figure 3.8 B). The baseline hump is not observed and most peaks are modulated almost to the baseline. Ultimately, the superiority of the GC×GC is more pronounced when the raw chromatogram is converted to a contour plot (Figure 3.8 C). The 2D chromatogram of diesel fuel demonstrates unparalleled resolution and ordered structure. For example, spots in the GC×GC chromatogram (each representing one chemical) that share the same retention time in the first dimension (x-axis) co-elute in a conventional GC analysis; analytes that fall along the same diagonal line belong to the same family of compounds. Overall, the tested GC×GC system is well suited for the analysis and separation of complex mixtures, such as the middle distillate fraction of petroleum.

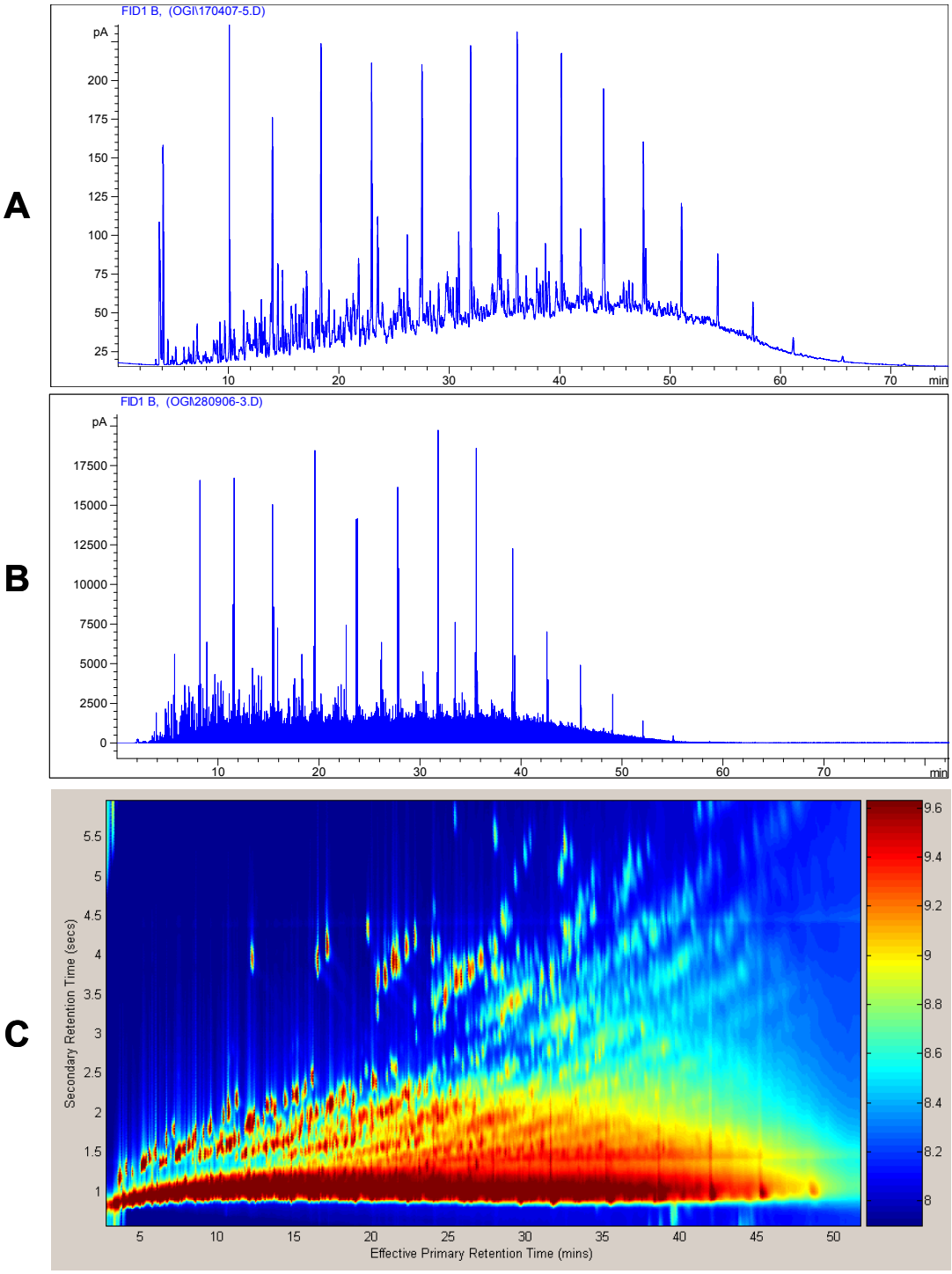

Figure 3.8. *Separation of diesel fuel. (A) 1D-GC analysis; (B) Raw GC×GC chromatogram of diesel fuel; (C) 2D contour plot, illustrating the improved resolution of this complex mixture (any compounds falling along the same vertical line co-elute in 1D-GC) and the ordered nature of the chromatogram (analytes falling along the same diagonal line belong to the same homologous family of compounds).*

Experiments designed to determine the range of volatilities that can be efficiently modulated were considered of equal importance. For these evaluations, a window-defining standard consisting of *n*-alkanes ranging from C_8 to C_{40} was used. Figure 3.9 B illustrates that the original trapping capillary (3 μm PDMS film thickness) was not suitable for modulating compounds with volatilities below that of the C_{27} *n*-alkane (marked). When compared to the 1D-GC analysis of the same standard (Figure 3.9 A), the raw GC×GC chromatogram displayed detrimental peak broadening for alkanes eluting after C_{27}. As previously discussed, peak broadening in the first dimension is indicative of excessive retention in the interface. In this particular instance, analytes with high boiling points could not be efficiently desorbed from the 3 μm trap because the desorption temperature (325 ˚C) was insufficient. Increasing this temperature was not a practical solution, as it promoted the destruction of the PDMS film. Unfortunately, the upper modulation limit reported in Figure 3.9 B represented only the beginning of the volatility range of the semi-volatile organic fraction of aerosols analyzed in the Berkeley laboratory. Accordingly, traps with extended volatility ranges were developed.

The two parameters that permit flexibility with respect to the volatility range of analyzable compounds are stationary phase film thickness and desorption temperature. For example, when the hairdryer was operated at the hot setting, the original interface (3 μm PDMS) could trap and release analytes with volatilities similar to C_{30} *n*-alkane. It was then predicted that a trapping capillary coated with a thinner film of PDMS would allow more efficient desorption of analytes with higher boiling points. Simultaneously, raising the temperature of the thinner film trap with

hot air from the blower could allow for the analysis of the least volatile compounds through elimination of cold spots. Experimental observations supported this hypothesis. A trapping capillary coated with a 1 μm stationary phase allowed effective modulation of *n*-alkanes up to C_{38}. Analysis of the same standard mixture with the application of hot air from the blower demonstrated that compounds with volatilities similar to n-tetracontane (*n*-C_{40}) could be efficiently modulated. In the next step, trapping capillaries were made of deactivated Silcosteel® tubing. Deactivated capillaries are coated with a very thin layer of stationary phase, and are commonly used upstream of the analytical column in order to retain undesired non-volatile analytes and matrix components. Evaluation of flattened deactivated tubing generated promising results when applied to the analysis of semi-volatile *n*-alkanes. Modulation of *n*-tetracontane was achieved regardless of the blower's air temperature; however, late eluting first dimension peaks appeared narrower when the *n*-alkane standard mixture was analyzed with the hot fan (Figure 3.9 C). This particular interface could not trap compounds with volatilities higher than that of *n*-C_{16}. Nevertheless, it is interesting to note that even the trap made of deactivated tubing exhibited a significant enhancement in sensitivity due to the previously discussed focusing effect (Chapter 1). The latest trapping capillary represents the simplest interface developed in this laboratory, and its applicability for the analysis of ambient air particulate matter is currently evaluated in Dr. Goldstein's laboratory.

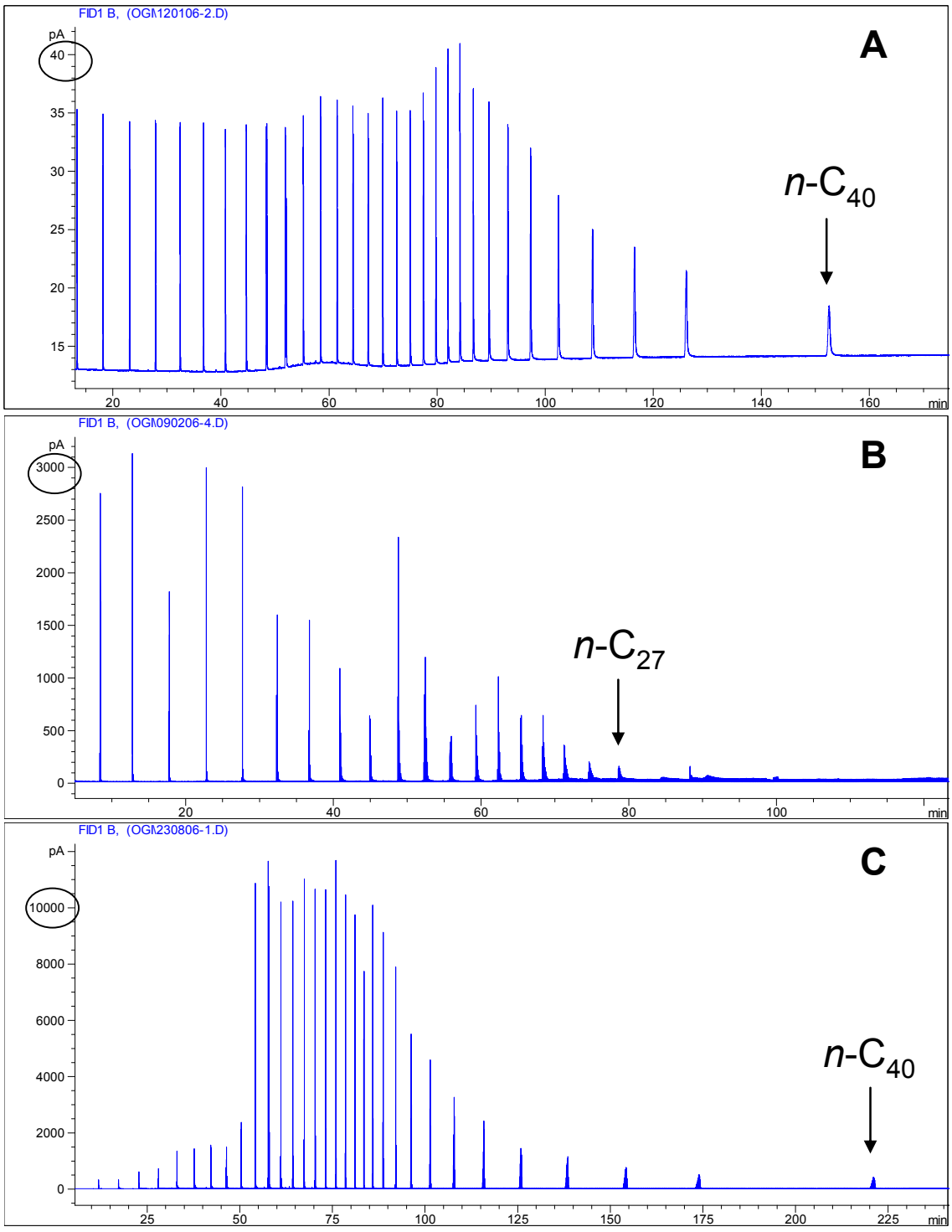

Figure 3.9. *Analysis of n-alkane standard (C_8 - C_{40} in chloroform) to define the range of volatilities that can be modulated. (A) 1D-GC analysis; (B) GC×GC analysis with a 3 µm PDMS film trap, the blower at the cool setting, and a split ratio of 5:1; (C) GC×GC analysis with a flattened deactivated guard Silcosteel® trapping capillary, the blower operated at the hot setting, and a split ratio of 2:1. Gains in sensitivity with the GC×GC method are circled.*

The choices of stationary phase film thickness and blower temperature not only determine the working volatility range of the modulator, but provide great flexibility during method development. Figure 3.10 summarizes the trapping potential of each interface prototype as a function of stationary phase film thickness. For each trap, results generated with the cold and hot blower were combined. The trapping capillary coated with a 1 μm thick stationary phase can be classified as a universal trap, as it is capable of modulating compounds with the widest volatility range (pink range in Figure 3.9). Accordingly, this interface was utilized for many applications presented in the next chapter, including field analysis of particulate matter ($PM_{2.5}$).

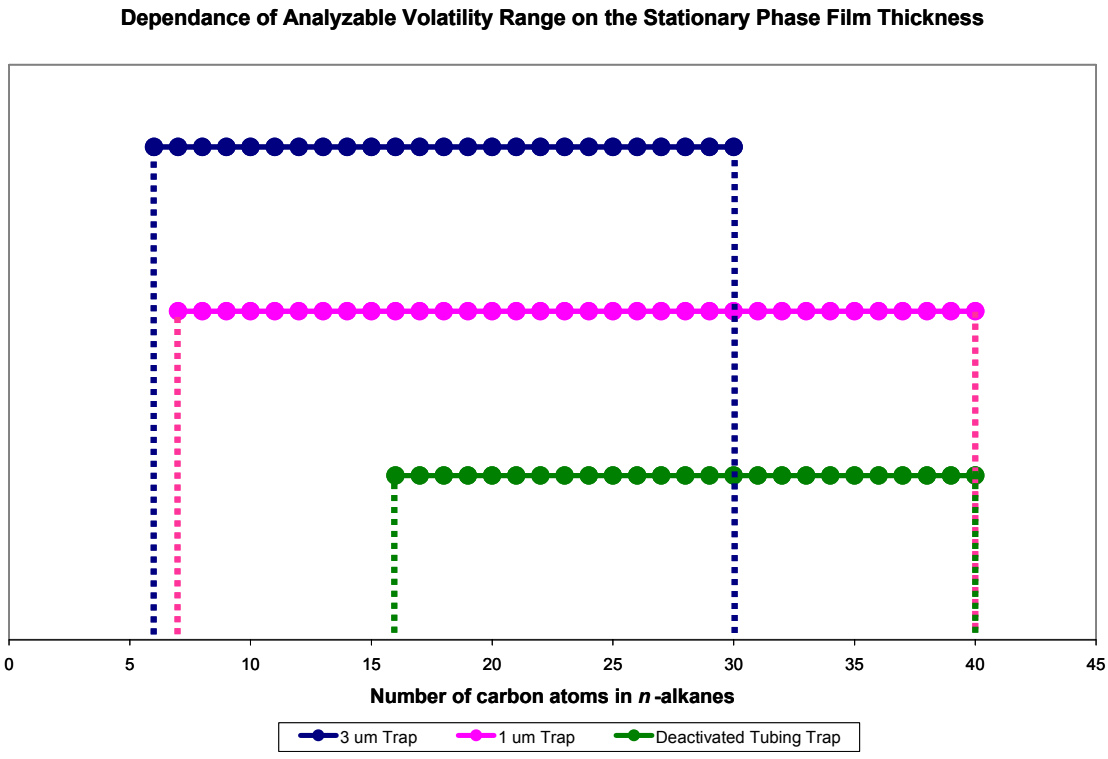

Figure 3.10. *A graph illustrating the volatility ranges of the interface prototypes as a function of stationary phase film thickness. For each trapping capillary, compounds from the most volatile range were trapped by employing the vortex cooler, while the least volatile fraction was trapped with the hairdryer set on hot.*

A closer examination of Figure 3.10 indicates that the analysis of volatile compounds with the thick (3 μm) and thin (1 μm) film traps is comparable. However, this small difference is very significant. Analysis of gasoline with the 1 μm trap is not feasible for the most volatile compounds, even with the vortex cooler set at –20 ˚C (Figure 3.11 A). Analyte breakthrough was observed as a vertical band in the contour plot at approximately 4 minutes. Modulation of gasoline was possible when the same conditions were applied to the thick film trapping capillary (Figure 3.11 B).

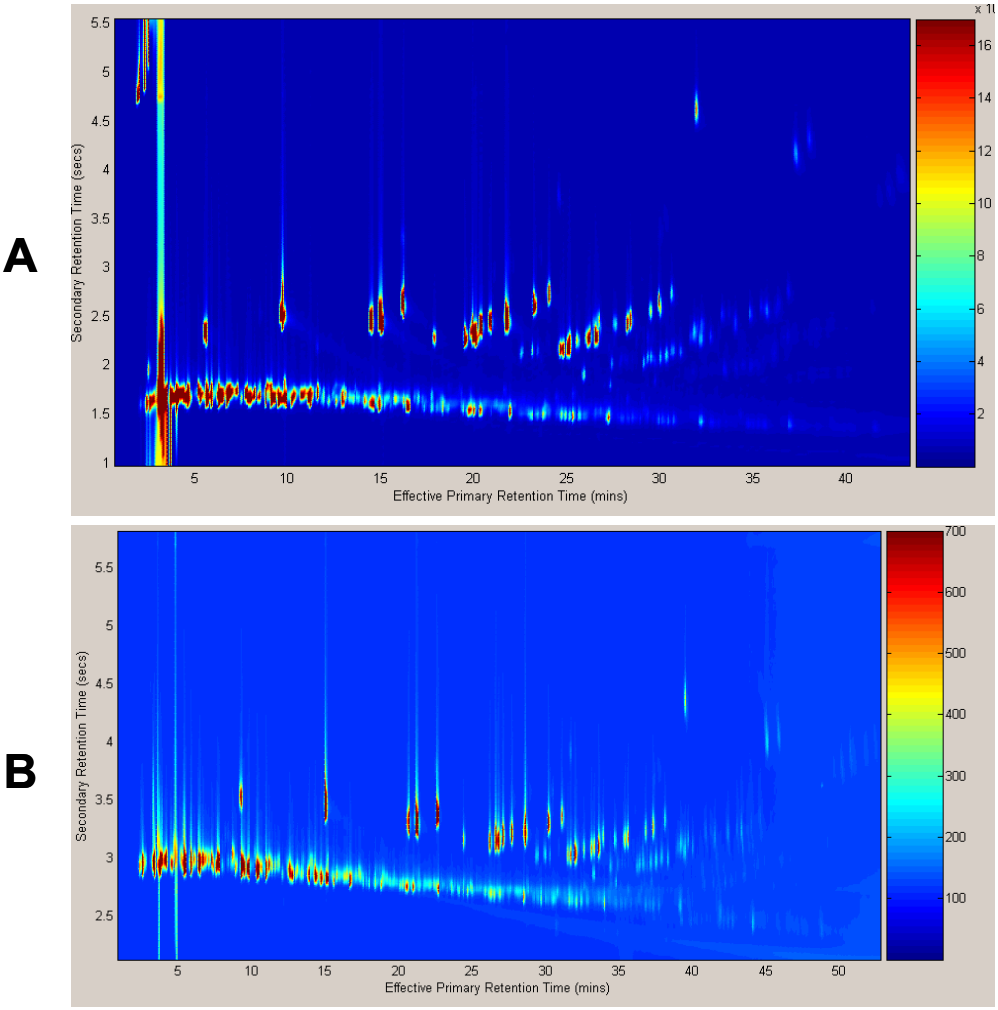

Figure 3.11. *GC×GC analysis of gasoline with the vortex cooler set at -20 ˚C with (A) thin film trap (1 μm); and (B) thick film trap (3 μm).*

Separation of volatile mixtures has traditionally been carried out with GC×GC instruments equipped with cryogenic modulators. Even in this category, only those utilizing liquid N_2 were demonstrated to be suitable for the separation of gasoline [13,14]. In the analyses carried out with liquid CO_2 interfaces, modulation of compounds with boiling points below that of *n*-octane was never reported [11,12,15]. In comparison, the interface developed in this laboratory was able to efficiently modulate analytes with volatilities similar to n-hexane without any cryogenic consumables. This accomplishment is not only a significant achievement in heater-based modulator design, but a milestone in the GC×GC field.

Finally, the proposed interface is also characterized by low operational and manufacturing costs. Table 3.4 presents a comparison of the operational costs of the modulator developed vs. commercially available interfaces that require cryogenic consumables. The methods used in calculating the anticipated costs can be found in the Appendix. In sum, the proposed interface represents one of the most affordable GC×GC systems capable of laboratory and field analysis of volatile and semi-volatile mixtures.

Table 3.4. *A comparison of the projected operational costs for the proposed interface and commercially available cryogenic GC×GC instruments.*

Interface	Daily Cost (USD)	Monthly Cost (USD)	Annual Cost (USD)
LECO Corp. (liquid N_2)	$ 100	$ 2 000	$ 24 000
Thermo Electron Corp. (liquid CO_2) [15]*	$ 6.34	$ 126.72	$ 1 520.64
Proposed interface (with vortex cooler)	33.75 ¢	$ 6.75	$ 81.01

* The projected cost of this interface is comparable to other liquid CO_2 modulators (i.e. LMCS).

3.5 Conclusions and Future Considerations

In spite of early criticism of heater-based thermal modulators by many experts in the field, the interface developed demonstrates great potential to once again play an active role in GC×GC applications. Inventions during the developmental stages of this research successfully eliminated the traditional drawbacks of heater-based modulators. In particular, narrow injection bands and second dimension peak widths, as well as the ability to efficiently modulate volatile mixtures, suggest on-par performance with at least some cryogenic interfaces. The simple and cost-effective operation of the interface, devoid of moving parts or cryogenic consumables, is an advantage that makes the modulator suitable for both laboratory and field analysis and monitoring applications. For example, on-site investigations of organic aerosols are currently conducted at the University of California in Berkeley (see Section 4). The benefits of the new modulator could also aid in the transition of GC×GC into a routine analytical tool. In essence, the presented research extends the boundaries set by present GC×GC interface technology.

It should be noted that while the proposed interface is currently considered a satisfactory prototype, further development and optimization will have to be pursued. First, the issue of robustness will have to be addressed, as this was noted to be a major drawback of the previous generation of resistively heated modulators. Not a single trapping capillary developed in this laboratory exhibited symptoms of degradation during operation; however, the separations carried out in this research are not representative of routine analysis. A long term study evaluating the robustness of the interface will be conducted by continuous operation of the interface

to modulate a simple *n*-alkane mixture (C_8 – C_{10} in hexane), injected repeatedly with an autosampler. This will be performed until the trapping capillary displays signs of degradation, as evaluated by performance parameters discussed in section 3.4. Secondly, a programmable blower design, analogous to oven temperature programming in a conventional gas chromatograph, should be considered. After examining Figure 3.10, it would be highly beneficial to gradually increase the temperature of the cooler during the GC×GC analysis. This would allow for the analysis of the widest range of analytes.

Harynuk and Górecki reported that the quality of modulation with thermal interfaces, measured by second dimension peak width and symmetry, depends on the ability to quickly heat and cool the trapping capillary [2]. With respect to the developed interface, decreasing the thermal mass (wall thickness) could enhance both heating and cooling rates. Commercially available thin-walled stainless steel tubing was recently purchased, treated and deactivated (Restek Corporation). In comparison to the presently utilized Silcosteel® tubing with a wall thickness of 0.13 mm, the thin-walled tubing has a measured wall thickness of 0.6 mm. This reduction in thermal mass should significantly increase the cooling rates and thereby permit not only shorter modulation periods, but possibly generate narrower injection bands and more symmetrical 2D peaks [16]. The anticipated drawback of utilizing thin-walled trapping capillaries is worse robustness, as these traps would be more fragile and could be damaged during handling.

This chapter described the design and development of a successful interface prototype. Selected applications utilizing the proposed modulator are described in

the next section. These include separations of semi-volatile compounds in ambient urban air, and various environmental samples, essential oils and petrochemical mixtures.

3.6 References

[1] Lee AL, Lewis AC, Bartle KDE, McQuaid JB, Marriott PJ (2000) J Microcol Sep 12(4):187-193

[2] Harynuk J, Górecki T (2002) J Sep Sci 25(5-6):304-310

[3] Williams BJ, Goldstein AH, Kreisberg NM, Hering SV (2006) Aerosol Sci & Tech, 40:627-638

[4] Goldstein AH, Williams BJ, Hering SV, Kreisberg NM, Panić O, Górecki T, Presented at the 7th International Aerosol Conference, St. Paul, MN, USA, Sept 10 – 15, 2006, abstract 12D5, page 475.

[5] Phillips JB, Liu Z (1991) J Chromatogr Sci 29(6):227-231

[6] Phillips JB, Ledford EB (1996) Field Anal Chem Tech 1(1):23-29

[7] Phillips JB, Gaines RB, Blomberg J, van der Wielen FWN, Dimandja J-M, Green V, Granger J, Patterson D, Racovalis L, de Geus HJ, de Boer J, Haglund P, Lipsky J, Sinha V, Ledford EB Jr. (1999) J High Resol Chromatogr 22(1):3-10

[8] Libardoni M, Hasselbrink E, Waite JH, Sacks R (2006) J Sep Sci 29:1001-1008

[9] Ranque GJ (1934) US Pat 1 952 281

[10] www.exair.com

[11] Marriott PJ, Ong RCY, Kinghorn RM, Morison PD (2000) J Chromatogr A 892(1-2):15-28

[12] Marriott P, Dunn M, Shellie R, Morrison P (2003) Anal Chem 75(20):5532-5538

[13] Harynuk J, Górecki T (2004) J Sep Sci 47:431-441

[14] Harynuk J, Górecki T (2003) J Chromatogr A 1019(1-2):53-63

[15] Beens J, Adahchour M, Vreuls RJJ, van Altena K, Brinkman ThUA (2001) J Chromatogr A 919(1):127-132

[16] Kaviany M, *Principles of Heat Transfer*, Wiley - Interscience, New York, 2001

4 Selected Applications

This section of the thesis focuses on the suitability of the GC×GC interface developed for resolving complex mixtures. The most notable among such applications is the analysis of organic compounds in urban air particulate matter ($PM_{2.5}$), currently conducted by Dr. Allen Goldstein at UC Berkeley. Other environmentally relevant analyses include those of polychlorinated biphenyls (PCBs) and a complex pesticide mixture. The GC×GC-FID separation of three selected essential oils is representative of analyses encountered with many natural samples. Finally, the GC×GC system developed was used to demonstrate simple and cost-effective separations of the major fractions of crude oil.

4.1 Environmental Analysis

4.1.1 Air Analysis

The air that surrounds all living things and permits life on this planet is considered an extremely complex mixture. Recent research states that a large amount of organic constituents in the earth's atmosphere have not yet been directly measured [1]. What is known is that anthropogenic volatile organic compounds (VOCs) play an important role in the generation of urban photochemical smog [2]. The World Health Organization (WHO) recognizes that exposure to air particulate matter can have detrimental effects on human health [3]. Still, uncertainty exists with regards to the health effects of VOCs in urban air particulate matter, in part due to a lack of appropriate analytical tools [4].

Conventional gas chromatography hyphenated to mass spectrometry (GC-MS) is well suited for air analysis. Unfortunately, the number of chemical compounds in typical air samples overwhelms the peak capacity offered by even the best columns. The analytical process used in air analysis usually consists of collecting samples in the field, analyzing them with various GC columns and identifying and/or quantifying the analytes of interest with mass spectrometry, in many cases high resolution mass spectrometry. Such analytical methods are not only laborious and expensive, but have been shown to be insufficiently sensitive and/or representative.

Improved resolution, enhanced sensitivity, and informative contour plots, associated with comprehensive multidimensional gas chromatography have been extensively utilized by some researchers. In one of the most important applications of GC×GC, Lewis et al. illustrated the separation of more than 500 chemical species of VOCs from urban air samples (Melbourne, Australia) in a single run [5]. What was previously observed to be baseline noise in GC-MS was determined to consist of numerous air pollutants. The presence of aliphatic, carbonyl, and aromatic bands in regions of 1D baseline noise was established. Prior to this study, many of these compounds were not known to exist in the atmosphere [5]. The authors of the study thus demonstrated the potential of GC×GC for not only monitoring applications, but for discovery purposes as well. Due to the limited resolving power and sensitivity of conventional 1D-GC methods, researchers might have previously underestimated the contribution of some VOCs to urban air pollution [5].

Following this important finding, more studies have been reported. Hamilton and Lewis analyzed ambient air in urban centers (Leeds, UK) and identified ~147 substituted monoaromatic species [6]. The authors noted that analogous GC-TOF-MS analyses could only separate 8 to 15 of the targeted analytes. In another study, GC×GC-FID and GC×GC-QMS were utilized to identify target oxygenated polynuclear aromatic hydrocarbons (oxy-PAHs), compounds which are currently suspected of carcinogenic and mutagenic activity [7]. The chromatograms obtained from the urban air samples in Finland contained approximately 1 500 peaks, 10 of which were identified as the target oxy-PAHs and quantified accordingly (0.5 - 5.5 ng/m^3). Schnelle-Kreis et al. investigated the suitability of direct thermal desorption combined with GC×GC (DTD–GC×GC–TOF-MS) for the analysis of organic compounds in ambient aerosols [8]. The use of DTD as a sample introduction method eliminated solvent use, a characteristic drawback of traditional sample preparation methods. When compared to similar analysis with GC–TOF-MS, GC×GC-TOF-MS exhibited a 10-times increase in the number of peaks detected and produced highly structured chromatograms ideal for rapid screening purposes. This approach led to the detection of roughly 15 000 peaks in $PM_{2.5}$ from Augsburg (Germany), out of which approximately 700 compounds were identified [9]. A similar study conducted in London (UK) reported the separation of more than 10 000 compounds, ranging in functionality from alkanes to polyoxygenated species [10]. Finally, Parsi et al. combined a non-discriminating thermal desorption/pyrolysis system [11] with GC×GC-TOF-MS for the analysis of particulate matter from Ottawa, Ontario [12]. Their chromatograms illustrated

superior resolution of many low and high molecular weight compounds, without the need for any sample preparation procedures.

While all the aforementioned examples of air analysis represent significant advancements in analytical atmospheric chemistry, they are all in-laboratory separations of samples collected on filters in the field. However, it can be argued that the most representative results should be obtained from analyses performed on-site. Only one GC×GC study to date analyzed urban air in the field. Xu et al. performed on-site measurements of the volatile fraction of urban air in Crete, Greece [13]. In the volatility range analyzed with the instrumentation employed (representative of the range from *n*-C_7 to *n*-C_{14}), approximately 650 compounds were identified. No studies have reported on the field analysis of semi-volatile organic compounds in air particulate matter.

In contrast to the VOCs analysis by the reported GC×GC methods, semi-volatile organics in the atmosphere are part of secondary organic aerosols (SOAs). SOAs arise from one of the many oxidation pathways of atmospheric VOCs, and are characterized by low vapour pressures and functional groups rarely detected with gas chromatography (alcohols and carboxylic acids) [1]. Derivatization of such samples can enhance their detection; still, the chemical complexity of this atmospheric fraction is very high. For example, an alkane mixture consisting of compounds with no more than 20 carbon atoms can form approximately 100 000 constitutional isomers. The number of possible isomers further increases with heteroatom substitution, as in the case of alcohols found in SOAs [1]. The separation of gasoline (Figure 3.11 B) and diesel fuels (Figure 3.8 C) serve as illustrative examples of

sample complexity – diesel, as the less volatile fraction (due to the larger number of carbon atoms in the molecules) is considerably more complex than gasoline.

Evidently, the identification and characterization of secondary organic aerosols is a challenging and important task. Such studies would provide more insight into the fate of natural and anthropogenic VOCs in the atmosphere, and allow possible assessment of specific organic compounds involved in aerosol production. In the past, field measurements of semi-volatile organics in urban air particulate matter were conducted in Berkeley with a thermal desorption aerosol gas chromatograph system (TAG) [14]. This custom-designed instrument combines sample collection and preparation, chromatographic separation, and FID/QMS detection. Typically, aerosol collection on-site for a predetermined period of time is followed by thermal desorption of particulate matter ($PM_{2.5}$) and injection of the organic fraction onto the GC-FID/MS system. It should not be surprising that even with MS detection, the developed 1D-GC system is unsuitable for resolving the samples encountered in this type of analysis.

The GC×GC interface presented in the previous chapter was installed onto the TAG instrument. The upgraded GC×GC-TAG (2D-TAG) immediately displayed superior resolution when applied to standard mixtures of fatty acid methyl esters (FAMEs) and EPA method 8270 analytes, as illustrated as contour plots in Figure 4.1. Shortly thereafter, an ambient air sample was collected for ~ 2 hours and analyzed with 2D-TAG (Figure 4.2). Even on a rainy day, when the abundance of aerosols in the atmosphere was at its lowest, many trace level organics were resolved

and detected. It should be noted that the chromatogram shown represents the first ever on-site analysis of semi-volatile organics in air.

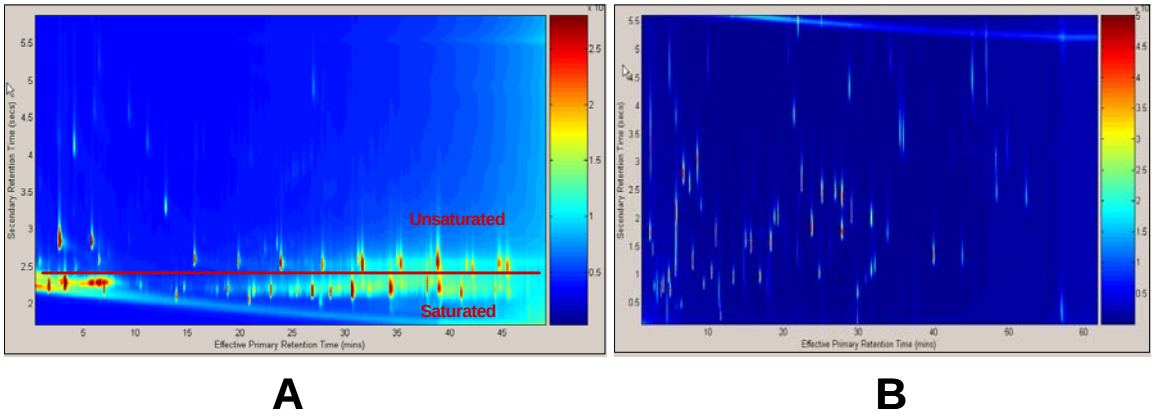

Figure 4.1. *2D-TAG analysis of (A) fatty acid methyl esters (FAMEs) – group-type separations are marked with the red line; and (B) EPA method 8270 analytes, a standard containing 116 of the most common air, water, and soil pollutants, including many polynuclear aromatic hydrocarbons (PAHs).*

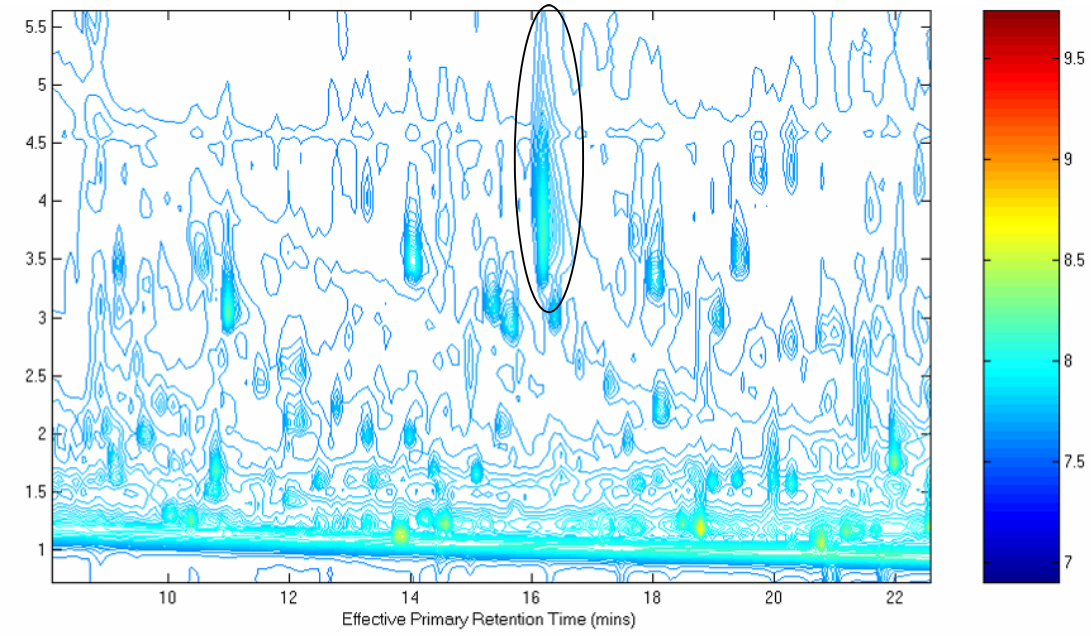

Figure 4.2. *2D-TAG analysis of an ambient air sample, collected on a rainy day, in Berkeley, CA, on January 29th, 2006. The circled peak can be attributed to wraparound.*

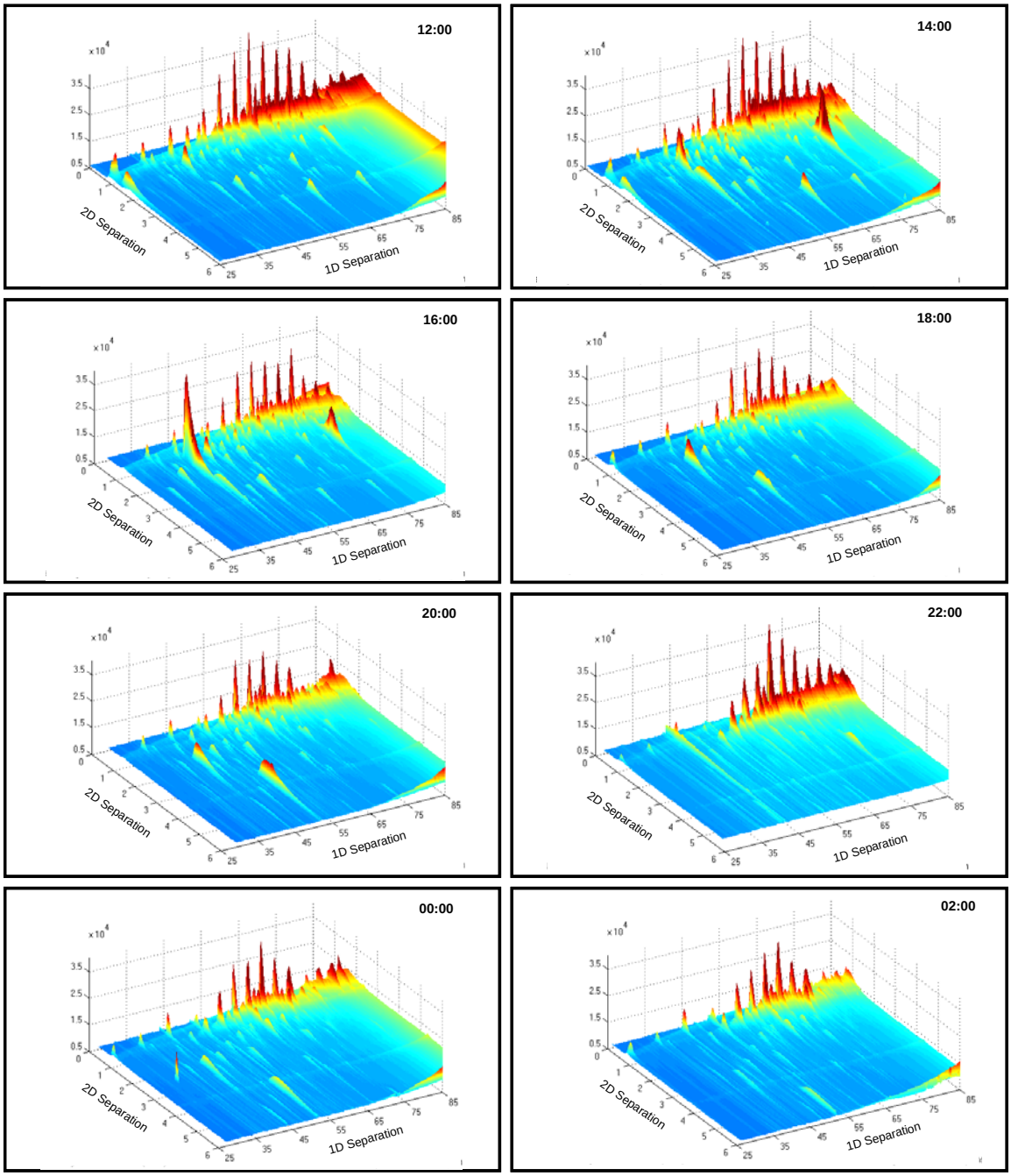

Figure 4.3. *On-site, time resolved 2D-TAG analysis of the semi-volatile organic fraction of urban air aerosols ($PM_{2.5}$) from Berkeley. The approximate time of sample collection is displayed in the upper right-hand corner of each chromatogram, altogether providing GC×GC resolution for a period exceeding 12 hours.*

Figure 4.3 presents the time-resolved analysis of the semi-volatile organic fraction of urban air aerosols from Berkeley, California [15]. A GC×GC chromatogram was generated following each 30 min sampling event of ambient air. This procedure was repeated every 2 hours in order to provide a 12 to 24 hour representation of the organic constituents in the atmosphere. Taking into account that 2D-TAG is a field instrument, both time- and space-resolved analysis of urban aerosols is possible. Only GC×GC-FID analyses are conducted at the present time; however, even these chromatograms are informative because the mere position of a compound in the 3D plot is indicative of its physical properties and chemical nature. In conclusion, this approach to investigations of ambient air aerosols is a pioneering step towards the GC×GC-assisted characterization of the semi-volatile fraction of urban $PM_{2.5}$.

4.1.2 Polychlorinated Biphenyls (PCBs) and Pesticides

Polychlorinated biphenyls (PCBs) are subject to bioaccumulation and biomagnification in the environment and are thus dangerous to wildlife and humans. Many of them are suspected carcinogens and mutagens [16]. For this reason, a tremendous amount of research has been conducted on these compounds not only by toxicologists, but by chromatographers as well. Confident assessment of PCBs in the environment requires a method capable of isolating and quantifying them in complex matrices such as food, soil and water.

PCBs exist as a mixture of 209 congeners, differing in the number of chlorine substituents and their substitution pattern on the benzene rings [16]. Although not all congeners are hazardous, the toxic ones are present in trace amounts and frequently co-elute with the more abundant and "less-dangerous" congeners in 1D-GC. In an effort to create a reliable method for PCB toxicity assessment, the WHO identified 12 PCB congeners (77, 81, 105, 114, 118, 123, 126, 156, 157, 169 and 189) as indicators of toxicity, due to their dioxin-like chemical behaviour [17]. Similarly, the European Union (EU) chose 7 PCB congeners (28, 52, 101, 118, 138, 153, and 180) to act as markers of harmful contamination [18]. Thus, depending on the regulations and standard operating procedures (SOPs) followed, the separation method applied must be able to identify and quantify at least a specific set of PCB congeners.

Presently, standard methods for the analysis of PCBs commonly require liquid chromatography (LC) pre-treatment in order to eliminate interferences from matrix components [19]. Following this, most samples require multiple GC-MS analyses for the identification of the specific groups of toxic congeners. The most efficient columns can only separate 7 out of the 12 WHO-recommended PCB congeners [19]. The entire process is expensive, time-consuming and labour-intensive.

Since no single column can separate all 209 PCB congeners in one run, GC×GC instrumentation has been applied in efforts to enhance the separation of this complex mixture. Harju et al. utilized GC×GC coupled with micro electron capture detection (μECD) to separate 194 PCB congeners in 240 minutes [20]. Focant et al.

recently separated 192 PCB congeners with GC×GC–TOF-MS in 146 minutes [18]. Among the baseline-separated PCBs were the 12 WHO-classified toxic congeners and the 7 EU marker PCBs. The latter approach is more desirable due to structural elucidation obtained from MS detection, as well as the decreased analysis time.

Comprehensive 2D-GC has also been used to for the separation and identification of PCBs from complex mixtures [17,21,22,23]. For instance, Korytár et al. applied GC×GC- μECD to rapidly screen for toxic PCBs and other chlorinated pollutants in cod liver samples [17]. Focant et al. compared quantitative aspects of GC×GC with ^{13}C-labelled isotope dilution (ID) TOF-MS (GC×GC–ID–TOF-MS) with conventional GC–HRMS [22]. The quantification of 4 marker PCBs spiked onto soil and sediment samples was comparable for both methods. However, the GC×GC approach benefited from minimal sample preparation, enhanced sensitivity (factor of 5-10), superior resolution, and lower instrumentation costs [23]. Following this, the authors utilized GC×GC-ID-TOF-MS for the separation and quantification of 18 toxic PCBs in food samples such as pork, fish and milk [23].

In addition to monitoring environmental samples for toxic PCB markers, there has recently been a growing interest in the application of GC×GC to the determination of chiral PCBs. Out of the 209 PCB congeners, 19 tri- and tetra-*ortho* congeners exist as atropoisomers at room temperature. These chiral PCB congeners are released into the environment as racemic mixtures [24,25]. Confident determination of non-racemic chiral PCB distribution in animal tissues and food extracts could provide crucial information relevant to biotransformations and selective bioaccumulation [26]. This type of analysis has posed considerable

challenges when 1D-GC separations were utilized. GC×GC studies reported improved resolution, enhanced sensitivity, and informative 3D plots of chiral PCBs in complex matrices, such as gray seal blubber, liver, brain and muscle tissues [27].

The interface developed in our laboratory was used to separate technical mixtures of PCBs. GC×GC-FID analysis of Arochlor 1245 (Figure 4.4 A), Arochlor 1260 (Figure 4.4 B), and a mixture of the two (Figure 4.4 C) indicates good resolution of many congeners that would co-elute in 1D-GC. Improvement in the separation and detection of the PCBs could be pursued by utilizing μ-ECD detection and a more suitable column set: separation based on volatility in the first dimension and separation based on planarity or chirality in the second (i.e. liquid crystal or cylcodextrin column, respectively) [21].

The analysis of transformer oil spiked with Arochlor 1245 in Figure 4.5 is representative of a PCB analysis in complex samples. Although mass spectral information was not available in this analysis, first and second dimension retention times and the overall pattern of the separated congeners could be used to quickly screen the petrochemical sample for the presence of PCBs. Potential PCB congeners in the oil were observed in the part of the chromatogram marked with the white border in the Figure. It is important to note that the extremely complex sample of transformer oil is representative of a semi-volatile matrix; therefore, this type of analysis would not be optimal with cryogenic interfaces.

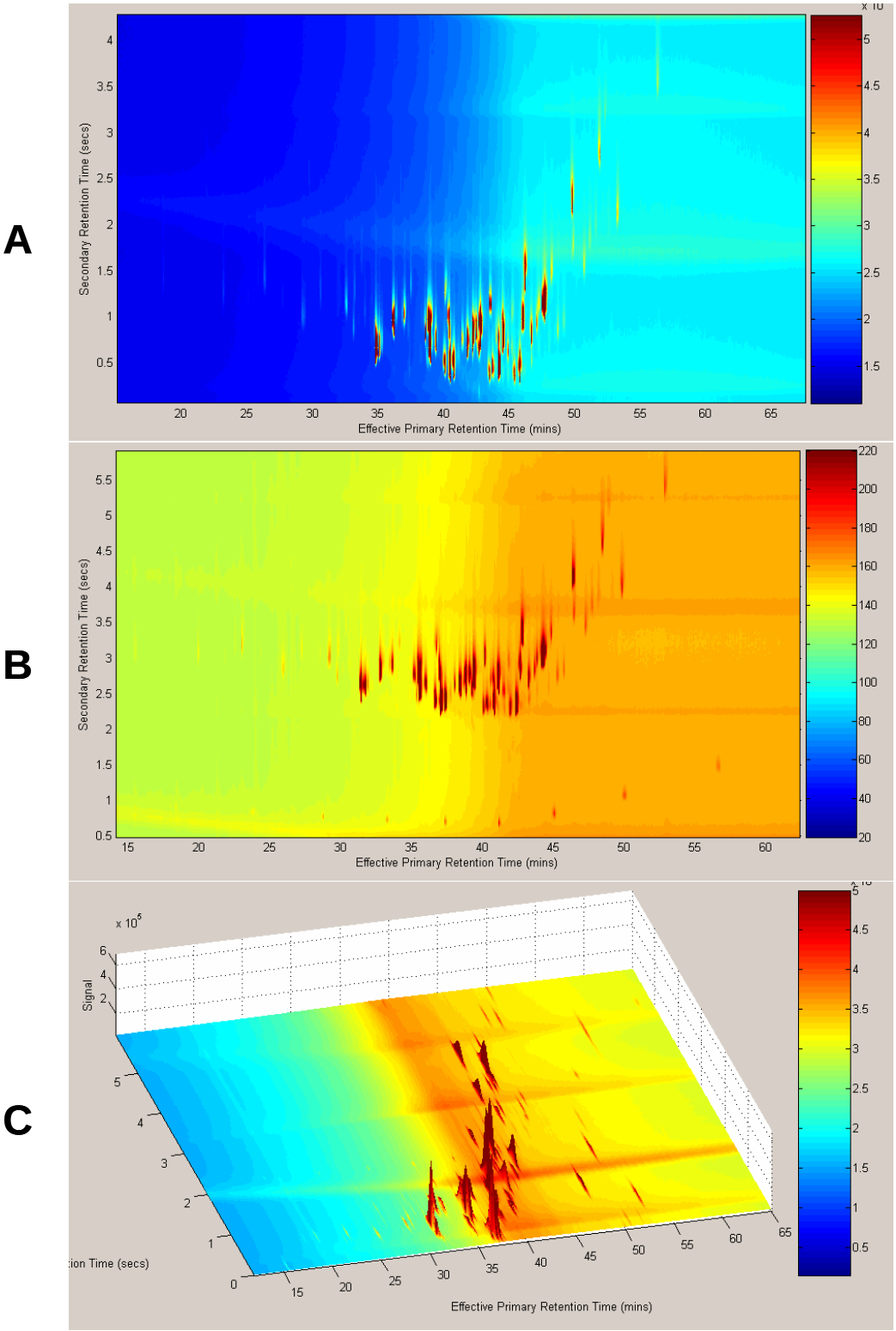

Figure 4.4. *GC×GC-FID analysis of PCB technical mixtures in splitless mode (A) Arochlor 1245; (B) Arochlor 1260; (C) a 1:1 mixture of Arochlor 1245 and 1260.*

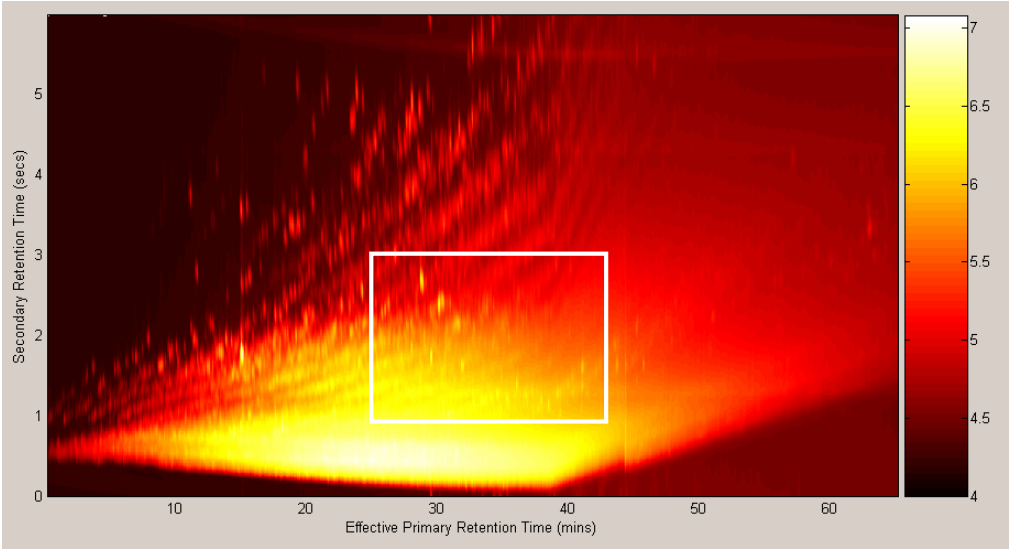

Figure 4.5. *GC×GC-FID analysis of transformer oil spiked with a technical mixture of Arochlor 1245 (splitless mode). The area containing suspected congeners is marked with the white box.*

Analysis of pesticides poses challenges to analytical chemists both with respect to sample preparation and chromatography. Similar to other toxic compounds, pesticides are usually distributed throughout the environment in trace amounts. Additionally, they are often found in extremely complex matrices such as food, soil and water samples. Rapid high resolution analyses of pesticides in natural samples are in high demand [28].

Traditional methods for pesticide analysis from food extracts require rigorous and time-consuming sample preparation methods, often generating large amounts of waste solvents. In an effort to eliminate matrix components as efficiently as possible, multiple solid-phase extractions (SPEs), LC pre-treatment, or liquid-liquid extractions (LLEs) are routinely applied [28]. In many cases, 1D-GC analysis following the aforementioned sample clean-up procedures still lacks the resolution to separate pesticides of interest from each other, as well as from the sample matrix.

The amount of published work dealing with the applications of GC×GC to pesticide analysis is relatively small, yet significant. Early applications to pesticide analysis in human tissues illustrated the method's potential for routine medical diagnostics. Liu et al. demonstrated baseline separation of 15 pesticides extracted from spiked human serum in less than 4 minutes [29]. Later, Dimandja et al. utilized GC×GC–FID for assessing pesticide exposure in children by analyzing small volumes of urine and serum [30]. The resolution of 16 pesticides in less than 4 minutes of analysis time was reported, a task that required more than one hour with the conventional GC-TOF-MS method. Determination of pesticides in food extracts is equally important. Using GC×GC–TOF-MS, Dallüge et al. separated and identified all 58 pesticides spiked onto celery and carrot extracts [31]. In this particular analysis, the pesticides that were not chromatographically resolved were successfully identified with the TOF-MS spectral deconvolution function.

The reported studies emphasize the importance of rapid and powerful methods for screening and monitoring of pesticides in food, water and tissues; however, the GC×GC instrumentation implemented is still very expensive to purchase and operate. The interface developed as part of this thesis significantly reduces operational costs and could, with a portable GC, be used for field analysis as well.

A complex technical mixture of the pesticide toxaphene was analyzed. Toxaphene is ubiquitously distributed in aquatic ecosystems [32]. Composed primarily of chlorinated bornanes, the pesticide mixture can theoretically consist of 32 768 different congeners. To date, approximately 246 congeners have been

detected, and multidimensional gas chromatography (MDGC) played a significant role in this challenging analytical task [32]. Results of GC×GC-FID analysis of toxaphene, carried out in our laboratory is presented in Figure 4.6 A. A close-up of a small part of the chromatogram reveals the extreme complexity of this technical mixture (Figure 4.6 B). Interestingly, even with the signal enhancement of the GC×GC modulator, many congeners were still approaching the FID detection limit. Nevertheless, the generated chromatograms produced satisfactory separations of a remarkably complex mixture. Future experiments, however, will likely require TOF-MS detection.

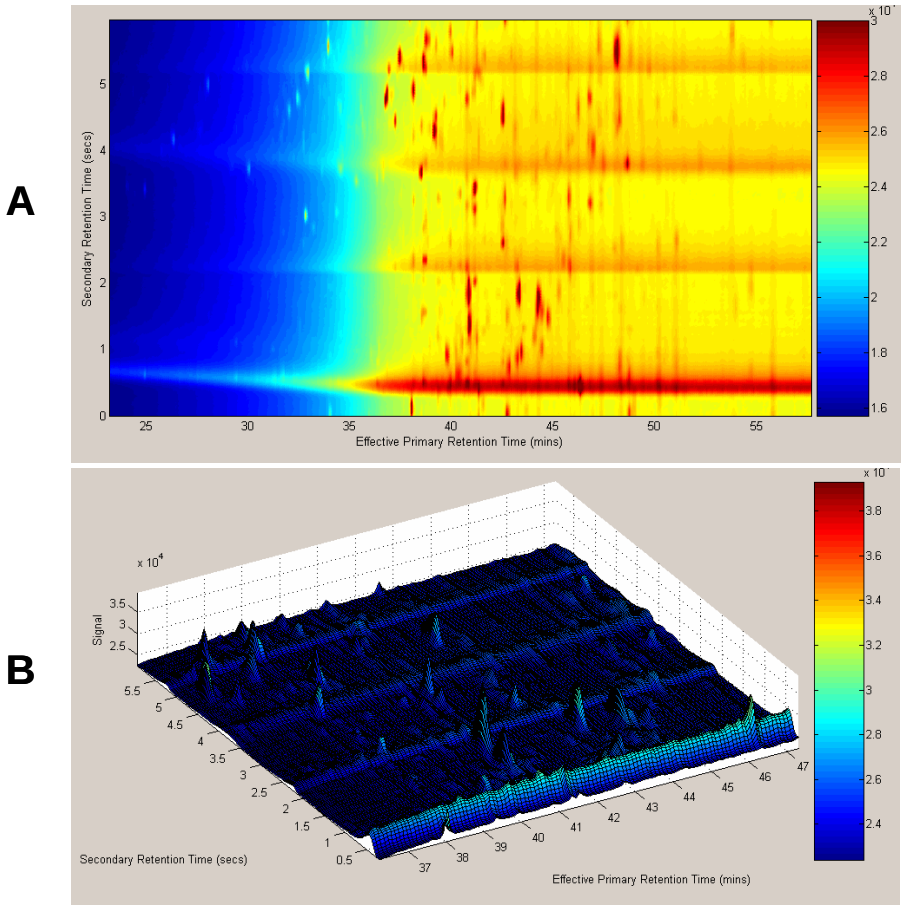

Figure 4.6. *GC×GC-FID analysis of the pesticide toxaphene in splitless mode (A); a close-up of a 10 minute time window illustrating the complexity of the sample near the chromatographic baseline (B).*

4.2 Essential oils

Derived from plants, essential oils are extensively used in the food and fragrance industries, and to a smaller extent for medicinal purposes. They are considered moderately to highly complex volatile mixtures that have typically been analyzed by gas chromatography [33]. The number of reported GC×GC applications for the high-resolution analysis and characterization of essential oils is steadily growing. A list of selected applications in this field is summarized in Table 4.1.

Table 4.1. *Selected GC×GC separations of natural essential oils. Adapted from [33].*

Essential oil(s)	**References**
Tea tree and lavender	[34,35,36]
Ginger	[37]
Peppermint and spearmint	[38]
Australian sandalwood	[39]
Hops	[40]
Coriander leaves	[41]
Traditional Chinese medicines (TCMs)	[42,43]
Eucalyptus	[44]
American and Asian ginseng	[45]
Tobacco	[46,47]

The GC×GC interface developed was applied for the separation of previously unreported essential oils. Figures 4.7 A, B and C represent GC×GC-FID analyses of rosemary, sage and neroli essential oils, respectively. The analyses point to yet another class of compounds that can be analyzed with the interface operated without cryogenic consumables. Future work in this area will focus on the characterization of individual components of the essential oils by replacing the FID with TOF-MS.

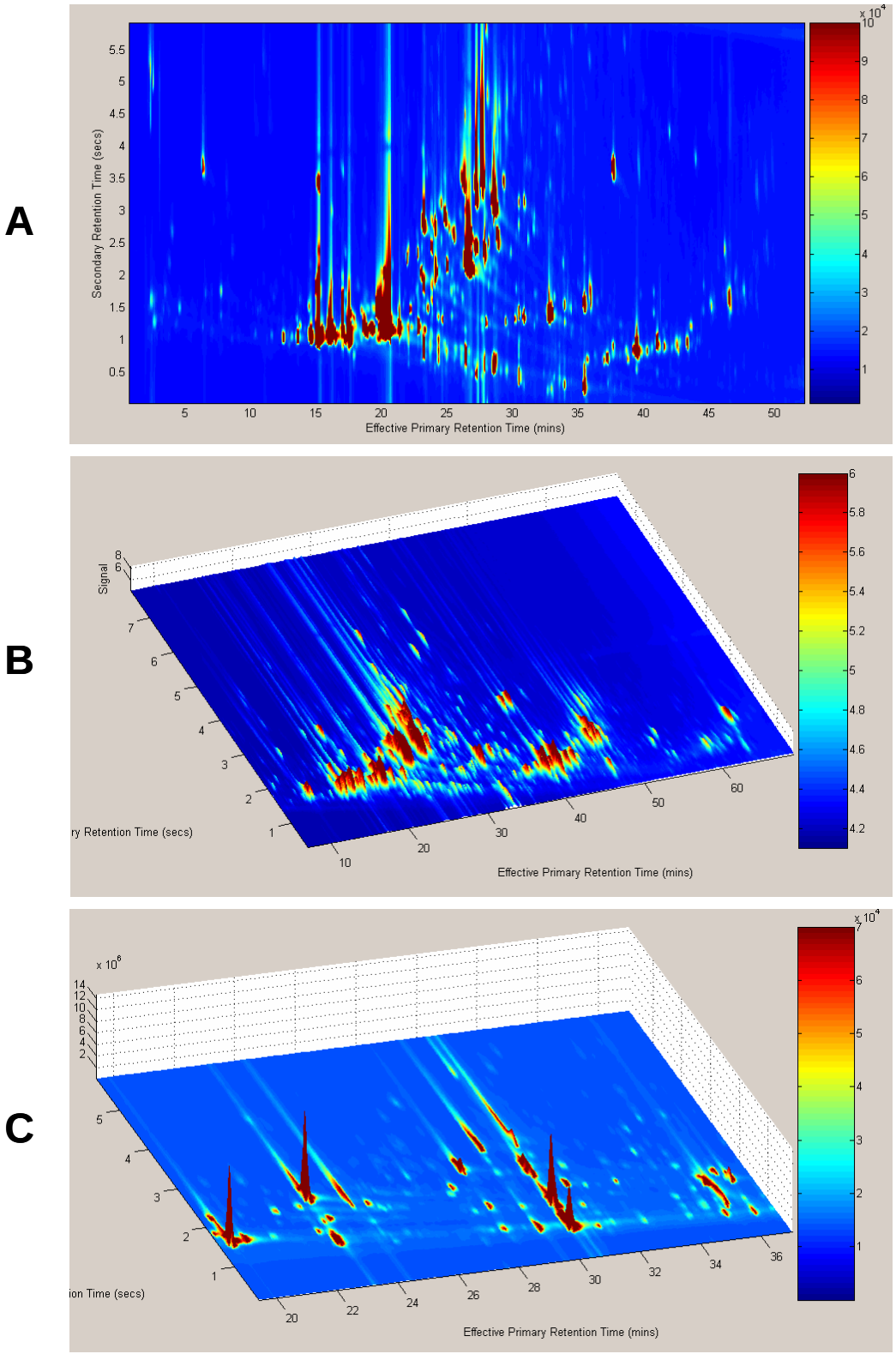

Figure 4.7. *GC×GC-FID analysis of undiluted 100% natural essential oils of (A) rosemary; (B) sage; and (C) neroli.*

4.3 Petrochemical Analysis

In the early stages of development, GC×GC had a tremendously positive impact on the analysis of petroleum products [48,49,50,51,52,53,54,55,56,57,58,59]. Typical petrochemical samples, such as gasoline, kerosene, diesel and various oils, might contain thousands of different compounds. Increased peak capacity, enhanced resolution and the ordered nature of GC×GC chromatograms improved both the qualitative and quantitative aspects of petrochemical analyses. Increased resolution power and peak capacity produced some of the best chromatographic separations ever, and allowed quantitative analysis of many previously undetected compounds in complex mixtures. Qualitatively, the highly ordered nature of GC×GC chromatograms offered structural elucidation of the different components in the various petroleum samples. For example, analyzing petroleum fractions with a GC×GC system allows for its separation into different homologous families, e.g. paraffins, naphthalenes and aromatics ranging from C_{10} to C_{17} [60]. In fact, in the early days of GC×GC any advances in the technology could be measured by simply observing improvements in 2D chromatograms generated from petrochemical samples. Presently, GC×GC combined with TOF-MS is one of the most important tools in the petrochemical sector, although less common detectors have also been tried. Examples include sulphur chemiluminescence detection (SCD) for identifying sulfur components of crude oil [61], and nitrogen chemiluminescence detection (NCD) for the detection of nitrogen compounds in diesel fuel [62].

GC×GC instrumentation trends in the petrochemical industry closely followed the historic developments in interface technology. As a result, many of the early separations were conducted with the rotating thermal modulator, while present systems are equipped with cryogenic interfaces. Valve-based modulation offers simple and affordable analysis of all petrochemical fractions [63]. This interface technology is, however, characterized by short modulation periods and relatively low signal to noise enhancement. Thus, it may not represent the optimal analytical tool for the separations encountered in the petrochemical sector.

The interface prototype presented in this thesis can be considered a viable alternative to much more complicated and expensive cryogenic GC×GC systems. Characterized by all advantages of thermal modulation, the proposed interface provides a simple and cost-effective approach to performing comprehensive 2D-GC separations of petroleum mixtures. Successful analysis of gasoline, the most volatile distillation product of crude oil, has already been demonstrated (see Figure 3.11 B). It is anticipated that routine industrial applications can financially benefit from cryogen-free analysis of volatile mixtures. The separation of kerosene, the distillation product immediately following gasoline, is demonstrated in Figure 4.8 A. Another advantage of the proposed interface over cryogenic counterparts is the ability to efficiently analyze semi-volatile petrochemical mixtures, such as high density fuels and oils. Examples in order of decreasing volatility include the separation of diesel fuel (see Figure 3.8 C), industrial-grade machining oil (Figure 4.8 B), and transformer oil (Figure 4.5).

Considering the variety of samples analyzed, it is evident that the interface developed can be applied for GC×GC separations covering a broad range of petrochemical distillation fractions. Ultimately, hyphenation with TOF-MS detection should be pursued for future analysis, as the additional information gained with this method might prove invaluable.

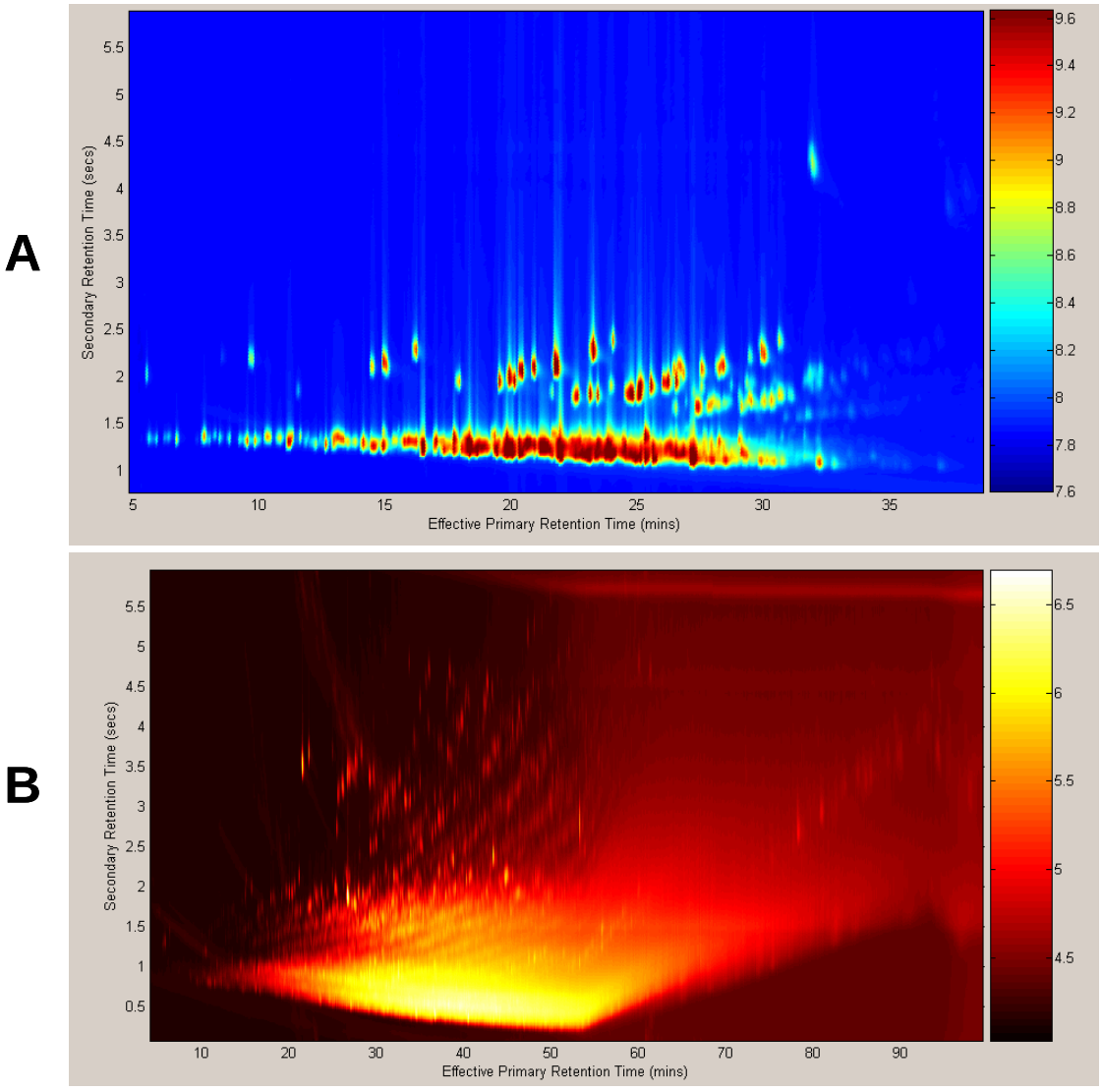

Figure 4.8. *GC×GC-FID analysis of petrochemical samples. (A) kerosene; (B) machining spindle oil , consisting of ~ 60% solvent-refined light paraffinic petroleum distillate and ~ 40% gas oil blend.*

4.4 Conclusions

The development of the interface presented in this thesis was initially intended to suit the type of analyses carried out in Dr. Goldstein's laboratory. Preliminary studies demonstrated the great potential of the interface developed in exploration of atmospheric aerosols. In the very near future, time-of-flight mass spectrometry (TOF-MS) will be incorporated into the high resolution time resolved analysis of urban air particulate matter. This will be an important step towards full characterization of the semi-volatile organic fraction of $PM_{2.5}$, an essential part of the atmosphere which is currently poorly understood.

While the simple and consumable-free approach to interface design enabled the on-site analysis of ambient air, initial evaluation of the interface (described in detail in Chapter 3) pointed to its applicability as a bench-top instrument suitable for a diverse range of applications. The performance of the interface prototype is on-par with some cryogenic models and its operational costs are dramatically lower (see Table 3.4). It is anticipated that the GC×GC system developed will be an alternative to commercial counterparts. For example, analysis of volatile mixtures (e.g. gasoline) in the absence of cryogenic consumables is economically feasible; additionally, high resolution separations of complex mixtures such as PCBs, pesticides, petroleum and natural samples are not only cost-effective, but simple to generate.

4.5 References

[1] Goldstein AH, Galbally IE (2007) Envr Sci & Tech 41(5):1514-1521

[2] Fowler D, et al. (1997) Fourth Report of the Photochemical Oxidants Review Group 75-104. UK Department of the Environment, Transport and Regions, London

[3] WHO (2003) Health Aspects of Air Pollution with Particulate Matter, Ozone and Nitrogen Dioxide, Bonn 2003

[4] Welthagen W, Schnelle-Kreis J, Zimmermann R (2003) J Chromatogr A 1019:233-249

[5] Lewis CA, Carslaw N, Marriott PJ, Kinghorn RM, Morrison P, Lee AL, Bartle KD, Pilling MJ (June 2000) Nature 405(15):778-781

[6] Hamilton JF, Lewis AC (2003) Atmos Environ 37:589-602

[7] Kallio M, Hyötiläinen T, Lehtonen M, Jussila ML, Hartonen K, Shimmo M, Riekkola M-L (2003) J Chromatogr A 1019:251-260

[8] Schnelle-Kreis J, Welthagen W, Sklorz M, Zimmermann R (2005) J Sep Sci 28:1648-1657

[9] Welthagen W, Schnell-Kres J, Zimmermann R (2003) J Chromatogr A 1019:233-249

[10] Hamilton JF, et al. (2004) Atmos Chem Phys 4:1279-1290

[11] Parsi Z, Górecki T, Poerschmann J (2005) J Chromatogr A 1019:251-260

[12] Parsi Z, Górecki T, Dabek-Zlotorzynska E, Ding L (2005) Chem Inz Ekol (Poland) 12:550-571

[13] Xu X, et al. (2003) Atmos Chem Phys 3:665-682

[14] Williams BJ, Goldstein AH, Kreisberg NM, Hering SV (2006) Aerosol Sci & Tech, 40:627-638

[15] Goldstein AH, Williams BJ, Hering SV, Kreisberg NM, Panić O, Górecki T, Presented at the 7th International Aerosol Conference, St. Paul, MN, USA, Sept 10 – 15, 2006, abstract 12D5, page 475.

[16] Schwarzenbach RP, Cschwend PM, Imboden DM (2003) Environmental Organic Chemistry, 2nd Edition. Wiley-Interscience, A John Wiley and Sons, Inc., Hoboken, New Jersey

[17] Korytar P, Leonards PEG, de Boer J, Brinkman UATh (2002) J Chromatogr A 958:203-218

[18] Focant J-F, Sjodin A, Patterson DG Jr. (2004) J Chromatogr A 1040:227-238

[19] Marriot PJ, Haglund P, Ong RCY (2003) Clin Chim Acta 328:1-19

[20] Harju M, Danielsson C, Haglund P (2003) J Chromatogr A 1019:111-126

[21] Haglund P, Harju M, Ong R, Marriott P (2001) J Microcol Sep 13(7):306-311

[22] Focant J-F, Reiner EJ, MacPherson K, Kolic T, Sjödin A, Patterson DG Jr., Reese SL, Dorman FL, Cochran J (2004) Talanta 63:1231-1240

[23] Focant J-F, Eppe G, Scippo M-L, Massart A-C, Pirard C, Maghuin-Rogister G, De Pauw E (2005) J Chromatogr A 1086:45-60

[24] Kaiser KLE (1974) Environ Pollut 7:93-101

[25] Schurig V, Glausch A, Fluck M (1995) Tetrahedron: Assymetry 6:2161-2164

[26] Bordajandi LR, Korytár P, de Boer J, José González M (2005) J Sep Sci 28:163-171

[27] Harju M, Bergman A, Olsson M, Roos A, Haglund P (2003) J Chromatogr 1019:127-142

[28] Geerdink RB, Niessen WMA, Brinkman UATh (2002) J Chromatogr A 970:65-93

[29] Liu Z, Sirimanne SR, Patterson DG Jr., Needham LL (1994) Anal Chem 66:3086-3092

[30] Dimandja J-M, Grainger J, Patterson DG Jr., Turner WE, Needham LL (2000) J Exp Anal Environ Epidem 10:761-768

[31] Dalluge J, van Rijn M, Beens J, Vreuls RJJ, Brinkman UATh (2002) J Chromatogr A 965:207-217

[32] de Boer J, de Geus H-J, Brinkman UATh (1997) Environ Sci Technol 31:873-879

[33] Adahchour M, Beens J, Vreuls RJJ, Brinkman UATh (2006) Trends Anal Chem 25(8):821-840

[34] Shellie R, Marriott PJ, Cornwell C (2000) J High Resol Chromatogr 23:554-564

[35] Shellie R, Mondello L, Marriott PJ, Dugo G (2002) J Chromatogr A 970:225-233

[36] Shellie R, Marriott PJ, Morrison P (2001) Anal Chem 73:1336-1347

[37] Shao YP, Marriott PJ, Shellie R, Hugel H (2003) J Flav Frag 18:5-13

[38] Dimandja J-MD, Stanfill SB, Grainger J, Patterson DG (2000) J High Resol Chromatogr 23:208-220

[39] Shellie R, Marriott P, Morrison P (2004) J Chromatogr Sci 42:417-422

[40] Roberts MT, Dufour J-P, Lewis AC (2004) J Sep Sci 27:473-445

[41] Eyres G, Dufour J-P, Hallifax G, Sotheeswaren S, Marriott P (2005) J Sep Sci 28:1061-1077

[42] Ruan Ch, Xu, G Lu X, Hua R, Kong H, Xiao K, Yong G (2003) Chromatographia Suppl 57:S-265-273

[43] Wu JF, Lu X, Tang WY, Lian XH, Kong HW, Ruan CH, Xu GW (2004) Chem J Chin Univ 25:1432-1444

[44] Zini CA, De Assis TF, Ledford EB Jr., Dariva C, Fachel J, Christensen E, Pawliszyn J (2003) J Agric Food Chem 51: 7848-7860

[45] Shellie R, Marriott P, Huie CW (2003) J Sep Sci 26:1185-1200

[46] Zhu Sh, Lu X, Dong L, Xing J, Su X, Kong H, Xu G, Wu C (2005) J Chromatogr A 1086:107-119

[47] Zhu Sh, Lu X, Xing J, Zhang Sh, Kong H, Xu G, Wu C (2005) Anal Chim Acta 545:224233

[48] Song SM, Marriott P, Kotsos A, Drummer O, Wynne P (2004) Forensic Sci Internatl 143(2-3):87-101

[49] Focant J, Reiner E, MacPherson K, Kolic , Sjödin A, Patterson DG Jr., Reese S, Dormand F, Cochran J (2004) Talanta 63(5):1231–1240

[50] Schoenmakers PJ, Oomen JLMM, Blomberg J, van Velzen G (2000) J Chromatog A 892:29–46

[51] Johnson KJ, Synovec RE (2002) Chemometrics Intell Lab Syst 60:225–237

[52] Venkatramani CJ, Phillips JBJ (1993) J Microcol Sep 5:511–516

[53] Blomberg J, Schoenmakers PJ (1997) J High Resol Chromatogr 20:539–544

[54] Frysinger GS, Gaines RB, Ledford EB Jr. (1999) J High Resol Chromatogr 22(4):195–200

[55] Frysinger GS, Gaines RB (1999) J High Resol Chromatogr 22(5):251–255

[56] Frysinger GS, Gaines RB (2001) J Sep Sci 24:87–96

[57] Beens J, Brinkman UATh (2000) Trends Anal Chem 19:260–274

[58] Prazen BJ, Johnson KJ, Weber A, Synovec RE (2001) Anal Chem 73:5677–5682

[59] Frysinger GS, Gaines RB (2000) J High Resol Chromatogr 23:197–201

[60] Beens J, Blomberg J, Schoenmakers P (2000) J High Resol Chromatogr 23, 182-188

[61] Marriott P, Shellie R (2002) Trends Anal Chem 21(9/10):573-583

[62] Bertsch W (2000) J High Resol Chromatogr 23(3):167-181

[63] Diehl JW, Di Sanzo FP (2005) J Chromatogr A 1086(1-2):115-121

Appendix

This section presents the economical analysis of selected cryogenically-assisted interfaces and the modulator developed in this laboratory. It should be emphasized that while effort was made to accurately reflect the operational costs, the true costs might deviate from the numbers given in the thesis because of the large variety of factors that might affect them.

The LECO Corporation manufactures and markets a GC×GC system that requires a constant supply of liquid N_2. At a minimum, this instrument's consumption rate is 50 L of liquid N_2 per day (figures as high as 100 L per day have been reported). Considering that the cost of the cryogen can be as low as $2 USD per liter [1] in academic settings, and assuming routine analysis over a 5-day working week and a 48-week year, the operating cost of this particular modulator would be $ 100 USD/day, $ 2 000 USD/month and $ 24 000 USD/year.

The Thermo Electron Corporation sells a dual-jet liquid CO_2 interface, initially designed and developed by Beens et al. [2]. The inventors report the cryogen consumption rate at a minimum of 2 kg per hour [2], while the price of liquid CO_2 is as low as $ 0.44 USD per kilogram [3]. Assuming routine analysis of 8 hours per day, 5 days per week, and 48 weeks per year, this particular interface would cost $ 6.34 USD daily, $ 126.72 USD monthly, and $ 1 520.64 USD annually to operate.

The interface developed in our laboratory does not require cryogenic liquids for GC×GC analysis. Instead, a commercially-available cooling blower based on the vortex tube technology is utilized. The model purchased requires a constant supply of pressurized air (70 – 100 psi) at a rate of 30 standard liters per minute (SLPM) to generate refrigeration of up to 514 kCal per hour [4]. The cost of generating the compressed air can be obtained from the cost of electricity. The Ontario Ministry of Energy reported the average cost of electricity for the year 2005 as 7.2 ¢ per kilowatt hour (kWh) [5]. The power requirements for the capacitative discharge power supply are negligible compared to the cost of the compressed air. Routine analysis is assumed to consist of 8 hours per day, 5 days per week, and 48 weeks per year. Accordingly, the interface developed is characterized by the following operational costs: 33.75 ¢ per day, $ 6.75 per month and $ 81.01 per annum. A sample calculation for the monthly expenditures is illustrated below.

$$Cost = \frac{\$0.072}{kWh} \times \frac{1kWh}{860.420kCal} \times \frac{504kCal}{hr} \times \frac{8hrs}{day} \times \frac{5days}{week} \times \frac{4weeks}{month}$$

$$Cost = \$6.75/month$$

References

[1] http://www.uark.edu/admin/busaffrs/scsp/nitrogen.html

[2] Beens J, Adachour M, Vreuls RJJ, van Altena K, Brinkman UATh (2001) J Chromatogr A 919(1):127-132

[3] http://www.bussvc.wisc.edu/purch/contract/wp5033.html

[4] http://www.exair.com

[5] http://www.energy.gov.on.ca/index.cfm?fuseaction=about.dashboard